12-14-2001

Reliability-Based Optimization of Anisotropic Cylinders with Response Surface Approximation of Axial Buckling Load

Bin Su

RELIABILITY-BASED OPTIMIZATION OF ANISOTROPIC CYLINDERS WITH RESPONSE SURFACE APPROXIMATION OF AXIAL BUCKLING LOAD

By

Bin Su

A Thesis
Submitted to the Faculty of
Mississippi State University
in Partial Fulfillment of the Requirements
for the Degree of Master of Science
in Engineering Mechanics
in the Department of Aerospace Engineering

Mississippi State, Mississippi

December 2001

RELIABILITY-BASED OPTIMIZATION OF ANISOTROPIC CYLINDERS WITH RESPONSE SURFACE APPROXIMATION OF AXIAL BUCKLING LOAD

By

Bin Su

Approved:

Masoud Rais-Rohani Associate Professor of Aerospace Engineering and Engineering Mechanics (Director of Thesis)	James C. Newman, III Assistant Professor of Aerospace Engineering and Engineering Mechanics (Committee Member)
Christopher D. Eamon Assistant Professor of Civil Engineering (Committee Member)	John C. McWhorter, III Head of the Department of Aerospace Engineering (Graduate Coordinator of the Department of Aerospace Engineering)

A. Wayne Bennett
Dean of the College of Engineering

Name: Bin Su

Date of Degree: December 14, 2001

Institution: Mississippi State University

Major Field: Engineering Mechanics

Major Professor: Dr. Masoud Rais-Rohani

Title of Study: RELIABILITY-BASED OPTIMIZATION OF ANISOTROPIC CYLINDERS WITH RESPONSE SURFACE APPROXIMATION OF AXIAL BUCKLING LOAD

Pages in Study: 70

Candidate for Degree of Master of Science

The reliability analysis and reliability-based optimization of laminated circular cylinders under axial buckling instability are studied. Structural reliability is measured in terms of Hasofer-Lind reliability index. The response surface models are used in both the calculation of the reliability index and the reliability-based optimization. In the reliability analysis, both deterministic and probabilistic sensitivity factors are investigated; the results show that the reliability index is most sensitive to the applied load and Young's modulus of the material. Two cases are considered in the optimization study. In the first case, the cylinder weight is minimized subject to a reliability constraint whereas in the second case, cylinder reliability is maximized subject to a weight constraint. In addition, two different optimization techniques are studied. In the first technique, a global response surface model of the buckling response based on 3000 Monte Carlo simulations is used for the design optimization whereas in the second technique, multiple local

regression models, with each based on approximately 20 simulations, are used in sequential search of an optimum design. An optimum design is found. The results based on sequential application of multiple local regression models are close to those from global optimization while the former is much more efficient in terms of computational cost.

ACKNOWLEDGMENTS

I would like to express sincere gratitude to the many people without whose selfless assistance this thesis could not have materialized. Sincere thanks are due to Dr. Masoud Rais-Rohani, my major professor, for expending time and effort to guide and assist me throughout this research work and for supporting me throughout this research work and the graduate program. Also, I would like to thank Dr. Christopher D. Eamon and Dr. James C. Newman for their valuable suggestions and comments.

I would like to extend my sincere appreciation to the NASA Langley Research Center for providing financial support under grant NAG 1-2038, and to the Department of Aerospace Engineering for providing financial support and computer facilities.

Last but not the least, I would like to thank all of those who helped to make this thesis possible, which includes my fellow colleagues and faculty members in the Department of Aerospace Engineering and Engineering Mechanics of Mississippi State University.

TABLE OF CONTENTS

LIST OF TABLES

LIST OF FIGURES

CHAPTER I

INTRODUCTION

Reliability Engineering

The study of reliability engineering is developing very rapidly worldwide. All areas from the electronics industry to the war industry, space aviation, and manufacture of mechanical and electrical products have attached great importance to it and carried out massive studies in this discipline.

Traditionally, structural design relies on deterministic analysis. Suitable dimensions, material properties, and loads are assumed, and an analysis is then performed to provide a more or less detailed description of the structure. However, fluctuations of the loads, variability of the material properties, and uncertainties regarding the analytical models all contribute to a generally small probability that the structure does not perform as intended. In response to the problem, methods have been developed to deal with the random nature of loads and material properties, and more recently, a general framework for comparing and combining these statistical effects has emerged. The methods have been used in application to structural design and reassessment of the safety of existing structures.

The question of reliability is important because of the ever-increasing demands on the increasing complexity of structures. These increased complexities may provide more

chances for the whole system to become faulty because of the failure of any related part, and the failure or fault in the whole system could threaten production, cause economic losses, and even jeopardize personal safety. In addition, the application of new materials or the adoption of new techniques may result in structures that are neither reliable nor safe. Furthermore, the high-performance demands and operation conditions of equipments can lead to mistakes in control and management. An optimal solution to these problems can not be found by deterministic means alone. The comprehensive engineering technology of reliability engineering has been developed to tackle these questions.

For a understanding of the concept of reliability, a strength-stress model of a component of a structure can serve as an example. To predict reliability of this component for which a failure occurs when the stress exceeds the strength, the nature of the stress and strength random variables must be known. Stress is used to indicate any component or equipment that tends to induce failure, while strength indicates any component or equipment that resists failure. Let the density function for the stress(es) be denoted by f_s and that for strength (r) by f_s as shown in Figure 1.1. The reliability is defined as the probability that the stress will not exceed the strength. The reliability is

$$R = P(r > s) = P(r - s > 0) \tag{1.1}$$

where P is the probability. The shaded region in Figure 1.1 is the interference region, which indicates a finite probability of failure. The magnitude of the failure probability is a function of the degree of overlap of the two distributions. The greater the shaded area, the greater the probability of failure.

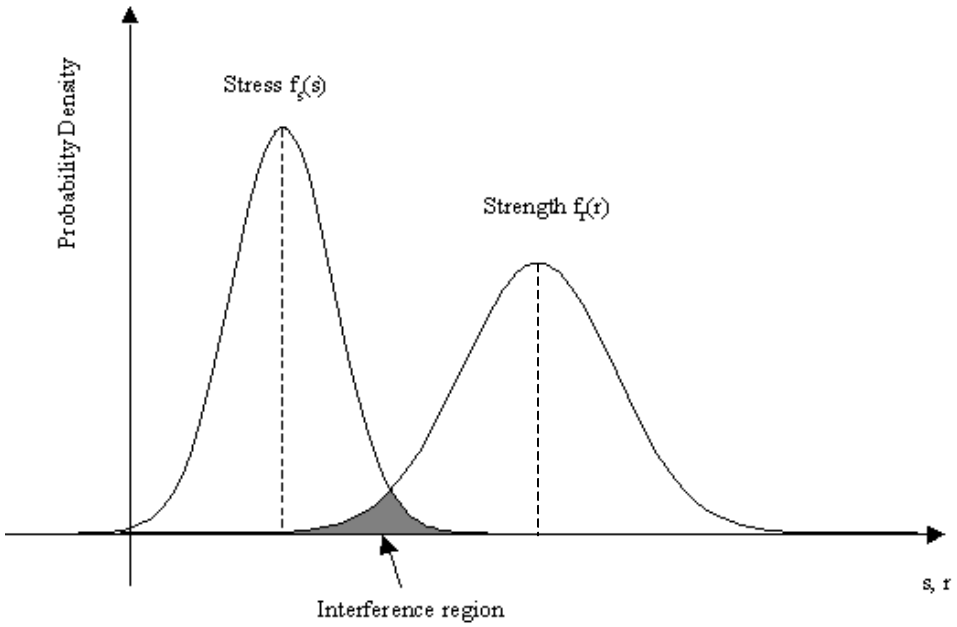

Figure 1.1 Stress, $f_s(s)$ and strength, $f_r(r)$ distributions with interference region

Reliability-Based Optimization

In the structural analysis of engineering design, there exists uncertainties in loading, material properties, geometry, and environmental conditions. These uncertainties should be taken into consideration carefully in order to ensure that the design performs its function within the desired confidence limit without failure. In robust design, it is important not only to achieve design objectives but also to maintain the robustness of design feasibility under the effects of variations caused by uncertainties.

In reliability-based plastic/elastic optimal design of mechanical structures, the problem is to find an optimal design point that is robust with respect to random variations of the structural parameters. Considering the (expected) construction costs, weight, volume, etc., denoted as $C=C(X)$, and the probability of failure of the structure, this goal can be achieved by solving an optimization problem of the following type:

Problem Type A

$$\min C(X)$$

s.t.

$$p_f(X) \le 1 - R \quad (R = \text{given reliability})$$

$$X \in D_0$$

Problem Type B

$$\min p_f(X)$$

s.t.

$$C(X) \le C_{\max}$$

$$X \in D_0$$

where D_0 is a given design space.

In solving problems of Type A or B or a certain combination of Type A and B, the main difficulty is the computation of the probability function and its derivatives. Moreover, the expected cost functions $C(X)$ and its derivatives must be computed.

Scope of the Present Study

The first part of this study is focused on the reliability analysis of laminated circular cylinders under axial buckling instability. Structural reliability is measured in terms of the Hasofer-Lind reliability index, which is based on a nonlinear response surface model of the buckling load. The effects of variations in material properties, geometric parameters, and applied load on reliability index are investigated using both

deterministic and probabilistic sensitivity factors. To assess the effect of anisotropy on buckling reliability, four discrete ply patterns are considered.

The second part of this study examines the reliability-based optimization of laminated circular cylinders under axial compression. Two cases are considered. In the first case, the cylinder weight is minimized subject to a minimum reliability constraint whereas in the second case the cylinder reliability is maximized subject to a maximum weight constraint. Results of weight minimization based on two different optimization techniques are compared. In the first technique, the buckling response of the cylinder over the entire design space is modeled by a single global nonlinear algebraic model derived from a large-scale Monte Carlo simulation. In the second technique, a point integration scheme is used to obtain multiple local linear response surface equations, using a much smaller data set, that are accurate over a small region of the design space. The results are found to be close, while the multiple local regression model technique is much more efficient than the global response surface technique.

Literature Review

Reliability Analysis

The area of structural reliability has grown at a tremendous rate in the past decades. Many methods have been proposed to investigate reliability, considering the type of problem, the parameters involved, and the uncertainty associated with these parameters. Uncertainties are typically modeled in terms of the mean (the central tendency), the variance (the dispersion about the mean), and the distribution. Various reliability estimation techniques use part or all of this information in different ways.

These variations give a particular method its own specific advantages and limitations. Two broad families of analysis methods for conducting the investigation have dominated the reliability and uncertainty analysis literature: analytical techniques and random sampling methods.

Analytical Techniques

This family consists of such techniques proposed by Hasofer and Lind (1974), Hohenbichler and Rackwitz (1987) among many others. All of these methods can be grouped into two types, namely, first- and second-order reliability methods (FORM and SORM). For FORM, the random variables are characterized by their first and second moments. Truncation of the Taylor's series expansion of the function forms the basis of this method. Higher moments, which might describe the skewness and kurtosis of the distribution, are ignored. For SORM, a higher order approximation for the failure probability computation is used because of the high nonlinearity of some limit state functions.

Shao and Murotsu[1] developed an approximate limit-state function by using a neural network. An "active learning algorithm" is proposed to enable the network to determine important failure regions by itself and also to do further learning at those regions to achieve a good fitness with the real structural state there.

Gucher and Bourgund[2] used an adaptive interpolation scheme to represent the system behavior by a response surface model. Subsequently, the response surface is utilized in conjunction with advanced Monte Carlo simulation techniques (importance sampling) to obtain the desired reliability estimates. Liu and Moses[3] used a sequential

response surface method together with Monte Carlo Importance Sampling to calculate the reliability. Based on their method, they developed a reliability analysis program RSM for aircraft structural systems.

Millwater and Wu[4] proposed a global/local method to reduce the computational requirements of probabilistic structural analysis. A coarser global model is used for most of the computations with a more refined local model used only at key probabilistic conditions. The global model is used to establish the cumulative distribution function (CDF) and the Most Probable Point (MPP). The local model then used the predicted MPP to adjust the CDF value.

Random Sampling Methods

This family of methods have been dominated by traditional Monte Carlo methods as well as numerous variations such as stratified sampling (e.g. Latin Hypercube Sampling), importance sampling and adaptive importance sampling.

Monte Carlo methods have a long history in reliability and uncertainty analysis as function integrators. The basic concept of Monte Carlo integration is to replace a continuous average by a discrete approximation for that average. However, Monte Carlo simulation or Latin Hypercube Sampling often require prohibitively large computational effort although the number of simulations is independent of the number of basic variables. Thus, in reliability and risk assessment, several more efficient and accurate calculation algorithms for analyzing complicated models have been proposed.

Wu[5] proposed an adaptive importance sampling (AIS) method that can be used to compute component and system reliability and reliability sensitivities. The AIS approach

uses a sampling density that is proportional to the joint probability density function of the random variables. Starting from an initial approximate failure domain, sampling proceeds adaptively and incrementally to reach a sampling domain that is slightly greater than the failure domain to minimize oversampling in the safe region.

Torng, et. al[6] proposed a robust importance sampling method (RISM) to calculate the reliability or its converse, the probability of failure. RISM first uses a tracking scheme to locate the failure domain. Next, an efficient adaptive sampling scheme is used to calculate the reliability with minimum computational effort.

Bucher[7] suggested an iterative Monte Carlo simulation procedure, which utilizes results from simulation to adapt the importance sampling density. He also reduced the statistical error of the estimated failure probability. His method is especially suitable for system reliability analysis since multiple failure modes need not be treated separately.

Computer Programs for Reliability Computation

Numerous computer programs have been developed by researchers to implement the FORM/SORM algorithms.

NESSUS(Numerical Evaluation of Stochastic Structures Under Stress), developed at the Southwest Research Institute[8] combines probabilistic analysis with a general-purpose finite element/boundary element code. Structural analysis is performed using the displacement method, the mixed-iterative formulation or the boundary element method, and the iterative perturbation is used for sensitivity analysis.

PROBAN (PROBability ANalysis)[9] was developed at Det Norske Veritas (Hovik, Norway). It was designed to be a general probabilistic analysis tool. PROBAN is

capable of estimating the probability of failure using the FORM or SORM. The approximate FORM/SORM results can be updated through importance sampling. The probability of general events can be computed by Monte Carlo simulation and directional sampling.

CALREL(CAL-RELiability)[10] is a general-purpose structural reliability analysis program designed to compute probability integrals. It incorporates four general techniques for computing the probability of failure: (1) FORM, (2) SORM, (3) directional simulation with exact or approximate surfaces, and (4) Monte Carlo simulation.

Khalessi, et. al[11] developed FEBREL (Finite Element-Based RELiability) as a general-purpose, probabilistic, finite element computer program at Rockwell International Corporation's Space System Division. They use the ANSYS general-purpose finite element computer program to provide the necessary computational framework for analyzing complex structures, while the FEBREL reliability computer program provides the basis for modeling, analysis of uncertainties, and computation of probabilities.

Estes and Frangopol[12] developed RELSYS (RELiability of SYStems) to compute the system reliability of structures modeled as a series-parallel combination of its components.

Reliability-Based Optimization

Reliability-Based Optimization in Structural Engineering

In deterministic structural optimization problems, the objective function is usually the volume or the weight of the structure and the constraints are related to code

requirements for stresses or displacements. A large number of numerical procedures have been developed to solve this type of problems. Most of the numerical algorithms used in deterministic structural optimization are based on sequential linear programming and dual methods. In reliability-based structural optimization, the total expected costs related to the structure such as weight can be used as the objective function. The constraints are reliability requirements connected with the possible failure modes of the structure.

Nikolaidis and Burdisso[13] used the concept of Hasofer and Lind to approximate the limit state function about the most probable point, and optimized a simplified aircraft wing model for system reliability. Torng and Yang[14] optimized a structure using an advanced reliability based optimization technique, and the reliability constraint was approximated linearly. Using the efficient safety index computation developed by Wang, et. al[15], they optimized frame and plate structures under the reliability constraint. Multipoint split approximations were used to approximate the reliability constraint. Chandu and Grandhi[16] integrated the general purpose structural reliability analysis program NESSUS with mathematical optimization capabilities for achieving optimal designs. They developed RELOPT (RELiability based structural OPTimization), an automated procedure for design optimization by integrating reliability analysis, sensitivity analysis, function approximations and data base management. Hendawi and Frangopol[17] presented a practical optimization approach to the design of both unstiffened and stiffened hybrid composite plate girders for highway bridges.

Tu, et. al[18] proposed a new approach called performance measure approach (PMA) in the reliability-based design optimization. They found the conventional

reliability index approach (RIA) and PMA are consistent in prescribing the probabilistic constraint. PMA is inherently robust and more efficient in evaluating inactive probabilistic constraints, while RIA is more efficient for violated probabilistic constraints.

Yang and Ma[19] developed an optimum design methodology based on reliability for a composite structural system. A two-level optimization is adopted. In system level optimization the structural total weight is taken as the design objective, and the requirement of system reliability is the constraint. In member level optimization the laminate reliability is taken as the design objective and keeping the weight or thickness of laminate constant is the constraint.

Response surface model in optimization

Sometimes the computation of optimization related structural analysis is very time-consuming, thus response surface models are used in optimization procedure. Response surface methodology (RSM) is a collection of mathematical and statistical techniques for solving problems in which the goal is to optimize the response Y of a system or process that is influenced by n independent variables X_1, X_2, …, X_n.

Liaw and DeVries[20] developed a reliability-based optimal design process by integrating reliability and variability analysis with optimization design processes using the response surface approach. They used the response surfaces for 'what-if' studies, optimization, robust design, and trade-off studies. Ragon and Haftka[21] used the response surface model for weight optimization of a composite stiffened panel. The response surface approximation is accomplished using the panel analysis/design code PASCO and

using response surface modeling techniques. Using a finite number of PASCO analysis/design computations, the optimal panel weight function is approximated by a quadratic polynomial over appropriate ranges of the loading and stiffness parameters. Sevant, et. al[22] proposed a partial differential equation (PDE) method to optimize the design of flying wings. They used response surface methodology to construct smooth analytic approximations of the noisy lift data. The combination of the PDE method RSM results in a design approach that is both efficient and robust.

Chapter II

RESPONSE SURFACE APPROXIMATION TECHNIQUE

Introduction

A response surface model is a algebraic model used to simulate the response of a system. The response surface model is developed using regression analysis. The input variables are called regressors or independent variables and the output is often called the response or dependent variable. To construct a response model, one needs to perform a number of simulations, then fit a response surface model using the least squares method based on these simulation results. After forming the response surface model, one can predict the system response for random values of independent variables within the domain of validity of the model.

The response surface technique has been used in both reliability analysis and structural optimization by other authors. In this study, this technique is used for a more efficient prediction of buckling response for the structural model. In performing reliability or optimization analysis, as many as several hundred or thousand buckling responses based on different values of random variables may be necessary. The shell analysis code used for buckling analysis takes approximately 4 minutes (Sun 350) for a single buckling calculation. Hence, the time spent on one reliability analysis or optimization run could easily exceed one day. When the response surface model is used

in lieu of the shell buckling analysis code, the reliability analysis or optimization takes a small fraction of that time without any significant loss in accuracy of predictions.

Response Surface Model/Linear Response Model

For a demonstration of the response surface and linear regression model, a simple example is given here. Suppose a system has two input variables X_1 and X_2, and a single output or response Y. The response variable Y is influenced by the values of the two input variables. We want to build a response surface model to simulate the actual response. The quadratic response surface model for this procedure is written as

$$\hat{Y} = \hat{\beta}_0 + \hat{\beta}_1 X_1 + \hat{\beta}_2 X_2 + \hat{\beta}_3 X_1^{\,2} + \hat{\beta}_4 X_2^{\,2} + \hat{\beta}_5 X_1 X_2 \tag{2.1}$$

where $\hat{\beta}_0, \hat{\beta}_1, \cdots$ and $\hat{\beta}_5$ are unknown constant coefficients. For a full quadratic model with n independent variables, there will be a total of $\frac{n^2+3n+2}{2}$ unknown coefficients in the model.

In a linear regression model for response variable Y in terms of X_1 and X_2, we can write

$$\hat{Y} = \hat{\beta}_0 + \hat{\beta}_1 X_1 + \hat{\beta}_2 X_2 \tag{2.2}$$

where $\hat{\beta}_0, \hat{\beta}_1$ and $\hat{\beta}_2$ are the three coefficients we need to find.

Suppose for the response surface model of (2.1) we have a set of n data points,

$$\begin{aligned} &Y_1, X_{11}, X_{12} \\ &Y_2, X_{21}, X_{22} \\ &\cdots \\ &Y_n, X_{n1}, X_{n2} \end{aligned} \tag{2.3}$$

The method of least squares is used to find the estimated values of $\hat{\beta}_0, \hat{\beta}_1, \cdots, \hat{\beta}_5$ in (2.1). That is, choose $\hat{\beta}_0, \hat{\beta}_1, \cdots, \hat{\beta}_5$ to minimize the sum of squares of the residuals

$$SS(\mathrm{Re}\,s) = \sum_{i=1}^{n} (Y_i - \hat{Y}_i)^2 \tag{2.4}$$

Many statistical software packages may be used for creation of the response surface models. SAS[23] was used in this study. The RSREG procedure in SAS is used for finding the coefficients in the full quadratic response surface models, and the REG procedure is used to do the same for linear regression models.

Candidate Designs/Simulations

To construct the response surface model, a number of candidate designs, including the input variables and the output are needed. We will use these data to fit the least square curve, i.e., the response surface. A series of random values for each variable are generated within specified limits for lower and upper bounds. These bounds define the region of validity for the response surface model.

For the reliability analysis and optimization using a single global buckling response model, a large number of Monte Carlo simulations were performed. In contrast, when using the sequential local response technique, the $n+1$ integration technique[24] (see Appendix C) was used, which requires only $n+1$ candidate simulations in constructing a locally-accurate response model, where n is the number of regressors.

Validation of Models

Before using a regression model, it is important to keep in mind that the model can only be used within its domain of validity. This domain is based on the limits specified by the lower and upper bounds on each random variable in performing the simulations. Besides the limits on the independent variables, there are several statistics that can be used to check the validity of the response surface model or linear regression model.

1. R^2

R^2 is defined as

$$R^2 = \frac{SSR}{SSTO} \tag{2.11}$$

where SSR is the regression sum of squares, i.e., the measure of the variation of the fitted regression values around the mean; SSTO is the total sum of squares, i.e., the measure of the variation of the observed values around the mean. R^2 measures the proportion of the variation of the candidate responses around the mean that is explained by the fitted regression model. The closer R^2 is to 1, the greater the degree of association between X's and Y. However, R^2 alone may not be a good measure of goodness-of-fit.

2. Root MSE

Many authors use the RMSE as a criterion for judging the accuracy of the model. The root mean square error (RMSE) is defined as

$$RMSE = \sqrt{\frac{1}{(N-p)}\sum_{i=1}^{n}(Y_i - \hat{Y}_i)^2} \tag{2.12}$$

where p is the number of parameters in the response surface or linear regression model, n is the number of candidate data points, Y_i are the candidate response values, and $\hat{Y}_i$ are the regression response values. A small RMSE means a good response surface or linear regression model.

3. t-test

This method is not often used in engineering because it is somewhat more complicated than the computation of RMSE and R^2.

First one must obtain an independent set of data (not the candidate data used to build the response surface). Let the independent set of data be defined as

$$Y_i^*, X_{i1}^*, X_{i2}^*, \cdots, X_{ip}^* \quad i=1, \ldots, m$$

Then, put $X_{i1}^* \cdots X_{ip}^*$ into the regression model to get

$$\hat{Y}_i^* = \hat{\beta}_0 + \hat{\beta}_1 X_{i1}^* + \cdots + \hat{\beta}_p X_{ip}^* \tag{2.13}$$

The prediction error at each point is estimated as

$$\delta_i = \hat{Y}_i^* - Y_i \tag{2.14}$$

Where the average $\overline{\delta}_i = \frac{1}{m}\sum_{i=1}^{m} \delta_i$ is a measure of the bias in using the model to predict Y_i^*.

To test for significant bias, test $H_0 : \mu_\delta = 0$ vs $H_1 : \mu_\delta \neq 0$. Use the t test:

$$t = \frac{\overline{\delta}}{\sqrt{s^2(\delta)/m}} \tag{2.15}$$

Reject H_0 if $|t| > t_{n-1,\alpha/2}$. Rejecting H_0 indicates significant bias.

Chapter III

RELIABILITY ANALYSIS OF COMPOSITE CYLINDRICAL SHELLS UNDER AXIAL COMPRESSION

Deterministic Buckling Analysis

For the calculation of axial buckling load N_{xcr}, the anisotropic cylindrical shell analysis code developed by Jaunky[25] is used. It is preferred to use this code because of its ease of modeling cylindrical shells. Because of the restrictions in this code, the circular cylinder was modeled as a semi-circular shell with symmetric boundary conditions along the two unloaded edges. The loaded edges were treated as clamped in this study.

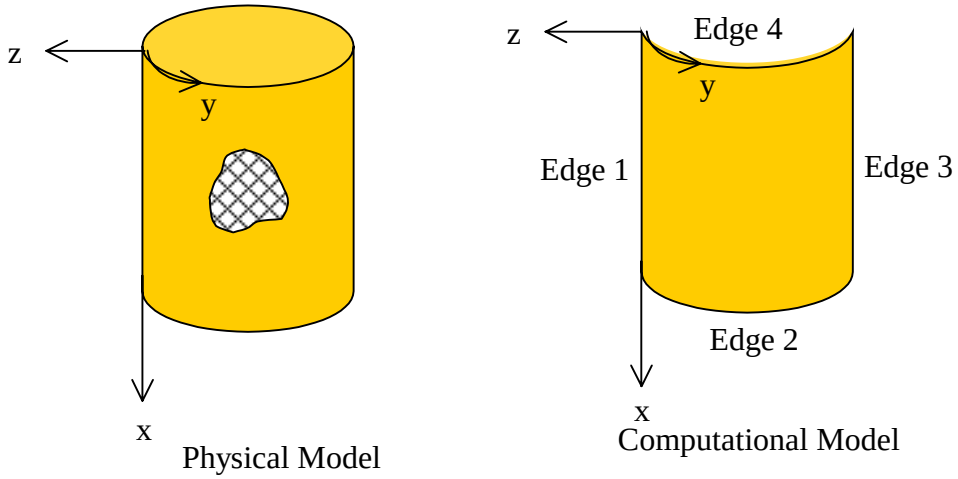

Figure 3.1 Circular cylinder and its corresponding computational model used for buckling analysis

The geometric and material properties of four types of cylinders are given in Table 3.1, where L is the cylinder length, D the cylinder diameter, and E_{11}, E_{22}, ν_{12} and G_{12} the material properties.

In defining the boundary conditions, the cylinder is allowed to undergo end shortening along edge 4 with edge 2 kept fixed. The condition of symmetry requires the v displacement and ϕ_y rotation to be kept zero along the unloaded edges of the model. All boundary conditions are specified in Table 3.2.

Table 3.1 Geometric and material properties for cylinder specimens

Specimen	L, in	D, in	t_{ply}, in	E_{11}, psi	E_{22}, psi	ν_{12}	G_{12}, psi
1	14	15.75	0.005	18.5780e6	1.64e6	0.0265	0.8737e6
2	14	15.75	0.005	18.6705e6	1.64e6	0.0264	0.8780e6
3	14	15.75	0.005	19.2588e6	1.64e6	0.0255	0.9057e6
4	14	15.75	0.005	18.6154e6	1.64e6	0.0264	0.8754e6

Table 3.2 Description of boundary conditions for the computational model[a]

Displacement	Edge 1	Edge 2	Edge 3	Edge 4
U	0	1	0	0
V	1	1	1	1
W	0	1	0	1
ϕ_x	0	1	0	1
ϕ_y	1	1	1	1

[a] 0 ≡ free, 1 ≡ fixed

Of the three options available in the shell analysis code, the strain-displacement relationship was modeled using Sanders-Koiter shell theory. The displacement function was represented by a Ritz approximation using Legendre polynomial interpolation functions. The buckling load is then found from an eigenvalue analysis.

For validation purposes, we compared the results of the shell code based on a 12^{th} degree Legendre polynomial interpolation function to those found using the finite-element code STAGS[26]. Here a mesh size of 51 x 169 quadrilateral elements was used, with the greater mesh density in the circumferencial direction.

Table 3.3 shows the computational predictions for the buckling force for four different cylinder specimens all with 16 layers but with different ply patterns. The buckling loads in all cases correspond to the first symmetric buckling mode. Specimen 2 with a quasi-isotropic ply pattern is found to be the strongest of the four examined. The errors in buckling load from the shell code are shown inside parenthesis, and they indicate that the shell code is based on a somewhat stiffer model of the cylinder. This error could be reduced using a higher-degree polynomial but at a significant increase in computational cost.

Table 3.3 Comparison of predicted buckling loads

		Axial Buckling Force, lb	
Specimen	Ply Distribution	Shell Code	STAGS
1	$[\pm 45/\mp 45]_{2s}$	111,349 (7.0%)	104,044
2	$[\pm 45/0/90]_{2s}$	185,420 (2.8%)	180,443
3	$[\pm 45/0_4/\mp 45]_s$	158,319 (2.4%)	154,655
4	$[\pm 45/90_4/\mp 45]_s$	167,717 (0.3%)	167,175

Probabilistic Buckling Analysis

The buckling load predictions in Table 3.3 assume no variability or randomness in any of the contributing parameters. However, variations in material properties, geometric parameters and loading could alter the buckling predictions, and a different picture may emerge when each parameter is assumed to be random with a particular mean and scatter such as those specified in Table 3.4. The statistical characteristics of the material in Table 3.4 correspond to AS4 12k/3502 (carbon-epoxy) unidirectional tape as specified in MIL-HDBK-17-2E[27]. The statistics associated with the geometric parameters (L, D, t and θ) are assumed in this case and are not based on any experimental observations. The ply pattern considered for the probabilistic buckling analysis is the same as that for specimen 4 in Table 3.3.

Table 3.4 Definition of random variables

Random Variable (No.)	Distribution Type	Mean	Coefficient of Variation (%)
L, in (1)	Normal	14	1
D, in (2)	Normal	15	1
t_{ply}, in (3-18)	Normal	0.005	1
θ_{ply}, deg. (19-34)	Normal	$[\pm 45/90_4/\mp 45]_s$	1
E_{11}, psi (35)	Normal	1.8e7	3.19
E_{22}, psi (36)	Normal	1.35e6	4.26
ν_{12} (37)	Normal	0.226	5
G_{12}, psi (38)	Normal	5.43e5	5.16

To determine the probabilistic buckling load, a Monte Carlo simulation was performed as described in Appendix B. For each simulation cycle, random values were generated for the 38 variables in Table 3.4. Note that each ply angle and ply thickness is treated as a separate random variable. The shell analysis code was used to find the buckling load in each cycle.

A total of 5,314 random experiments were conducted to determine the distribution, mean, and coefficient of variation of the buckling load. The histogram for the buckling load, P_{cr}, shown in Fig. 3.2, indicates a normal probability distribution with a mean of 151,203 lb and a standard deviation of 4,245 lb. In comparison, the deterministic buckling load with all random variables fixed at their corresponding mean values (see Table 3.4) is found to be 151,310 lb.

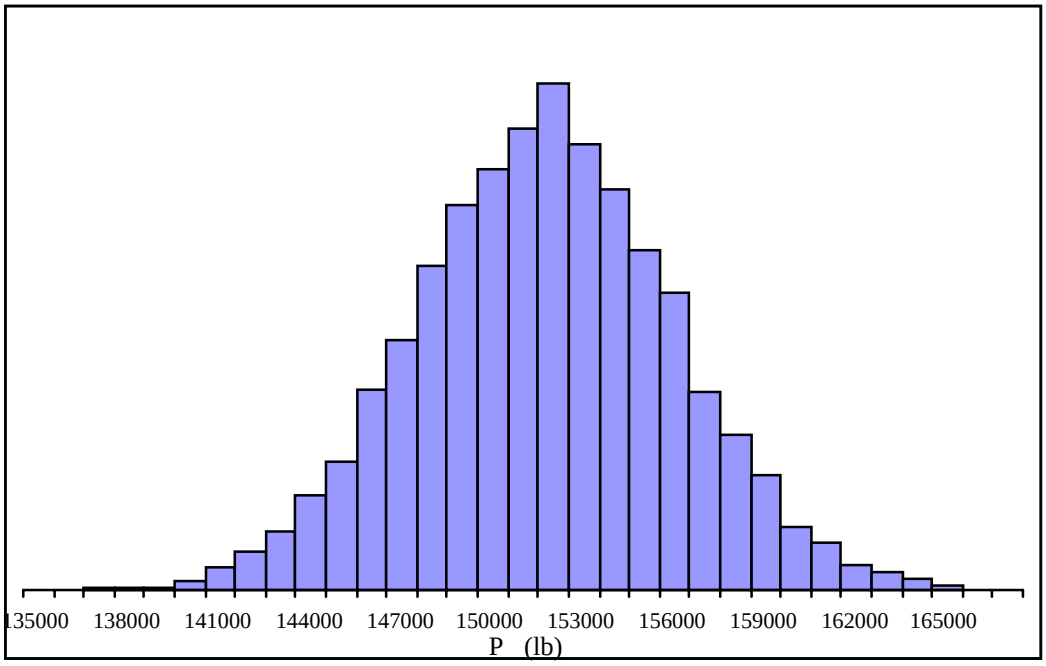

Figure 3.2 Histogram for buckling load, P_{cr}

The Monte Carlo simulations were performed for two reasons: (1) to measure the reliability of the cylinder by calculating the probability of failure directly from the results of the Monte Carlo simulation; (2) to estimate cylinder reliability by calculating the Hasofer-Lind index for which a regression model of buckling response based on these simulation data is used.

Structural Reliability Analysis

The limit state function for cylinder buckling is formulated as

$$g(X) = P_{cr} - P \tag{3.1}$$

where P is the applied axial force on the cylinder, P_{cr} is the corresponding buckling force, and X is the vector of random variables. According to Eq. (3.1), $g < 0$ means failure, $g > 0$ indicates safety, and $g = 0$ represents the limit state (surface separating the failure and safe regions). In this case, g is a function of 39 random variables, 38 of which are defined in Table 3.4 with the 39th variable being the applied load P, which is assumed to be normally distributed with an assumed mean of 143,690 lb and COV = 5%.

The structural reliability is estimated in terms of Hasofer-Lind reliability index with the corresponding probability of failure compared with that obtained from a direct Monte Carlo simulation.

Hasofer-Lind Reliability Index

The first-order second moment method developed by Hasofer and Lind[28] gives a measure of structural reliability in terms of the reliability or safety index β, which is

defined as the shortest distance between the origin of the reduced coordinate system and the failure surface defined by the limit state ($g = 0$) as shown in Fig 3.3.

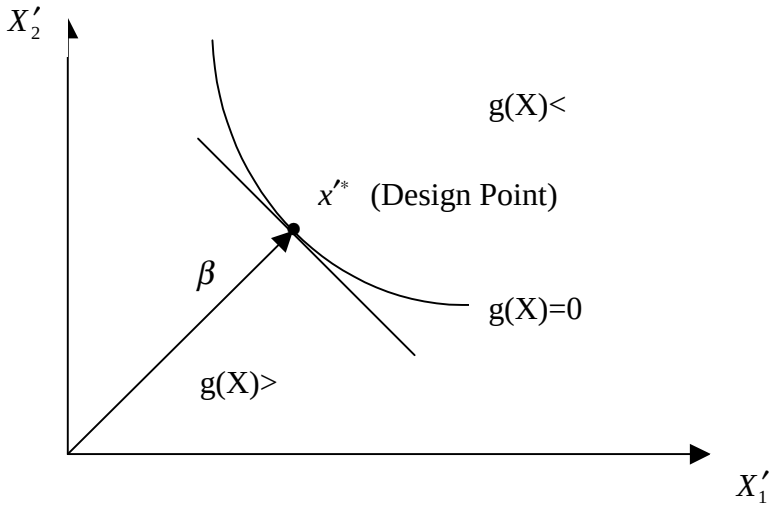

Figure 3.3 Hasofer-Lind reliability index: nonlinear performance function

The point on the failure surface corresponding to β is called the design point or the most probable failure point (MPP) with the coordinates defined as

$$x_i'^* = -\alpha_i^* \beta, \qquad i = 1,2,...,39 \tag{3.2}$$

with direction cosines given by

$$\alpha_i^* = \frac{\left(\frac{\partial g}{\partial X_i'}\right)_*}{\sqrt{\sum_{i=1}^{39}\left(\frac{\partial g}{\partial X_i'}\right)_*^2}}, \quad i = 1,2,...,39 \tag{3.3}$$

where x_i' corresponds to x_i in reduced coordinate system. When limit-state function is nonlinear, as is the case here, β is determined through an iterative procedure based on an initial estimate for the coordinates of MPP. This procedure is described in Appendix C.

The advantage of estimating reliability with the Hasofer-Lind approach is that it only depends upon the mean and variance (first and second moment properties) of individual random variables and not their distribution type[29]. The disadvantage is that, for non-normal random variables, accuracy is sacrificed. The probability of failure is directly related to β according to the relation

$$P_f = \Phi(-\beta) \tag{3.4}$$

where Φ is the cumulative distribution function (CDF) of the standard normal variate.

In applying the Hasofer-Lind reliability index approach to the problem of cylinder reliability, the limit state function defined by Eq. (3.1) must be expressed as $g(x_1', x_2', ..., x_{39}')$ with all uncorrelated and independent random variables transformed to the reduced coordinate system such that $\mu_{X_i'} = 0$ and $\sigma_{X_i'} = 1$. In Eq. (3.1), the limit state function is defined as the difference between the critical buckling load and the applied load with the buckling load being an implicit function of the 38 random variables (see Table 3.4).

Since the calculation of β is an iterative procedure, the buckling analysis code may need to be called hundreds of times for β calculation. Since one run of the buckling analysis code takes about 7 minutes using a Sun 350 microcomputer, a β calculation could take more than 24 hours. Thus for the sake of efficiency, instead of using the shell code directly in the calculation of reliability index, an algebraic response surface model

of the buckling load was used. Another advantage of this approach is an efficient calculation of sensitivity derivatives of the limit-state function with respect to individual random variables. The Monte Carlo simulation results found previously for the probabilistic buckling load were used to generate a second-order response surface model for the buckling load.

The equation for P_{cr} was generated rapidly using the SAS mathematical software based on the least squares technique. The resulting model is a full quadratic polynomial with a mean of 151,203 lb, root MSE of 150.85 and R^2 of 0.9989, which means the model will be quite good for prediction of P_{cr}.

For the cylinder in Table 3.4 with the specified loading condition, we get

$$\beta = 0.91$$

which corresponds to a probability of failure

$$\Phi(-\beta) = 0.181.$$

Monte Carlo Simulation

The limit state function is defined as

$$g = P_{cr} - P \tag{3.5}$$

We take g<0 as a failure due to buckling. P_{cr} is the buckling load calculated by the shell analysis code. The applied load P is the specified applied load.

Using the limit-state function formulation in Eq. (3.1) and the response surface model for the buckling load, a direct Monte Carlo simulation was performed. Specimen failure in buckling is detected when the limit state function g(x) = 0 is violated in an experiment. The probability of failure is then defined as

$$P_f = \frac{N_f}{N} \tag{3.6}$$

where N is total number of simulations and N_f is the number of failures. The coefficient of variation of failure probability found as

$$COV(P_f) = \frac{\sqrt{\frac{(1-P_f)P_f}{N}}}{P_f} \tag{3.7}$$

The same number of simulation cycles were run as before (5314) and 988 instances were found where $g < 0$. This resulted in a probability of failure of 0.186 for this specimen based on the assumed distribution, mean and scatter for the applied load, which is very close to what was obtained using Hasofer-Lind method. The plots of P_f and COV are shown in Fig. 3.4 with the final COV = 2.87%.

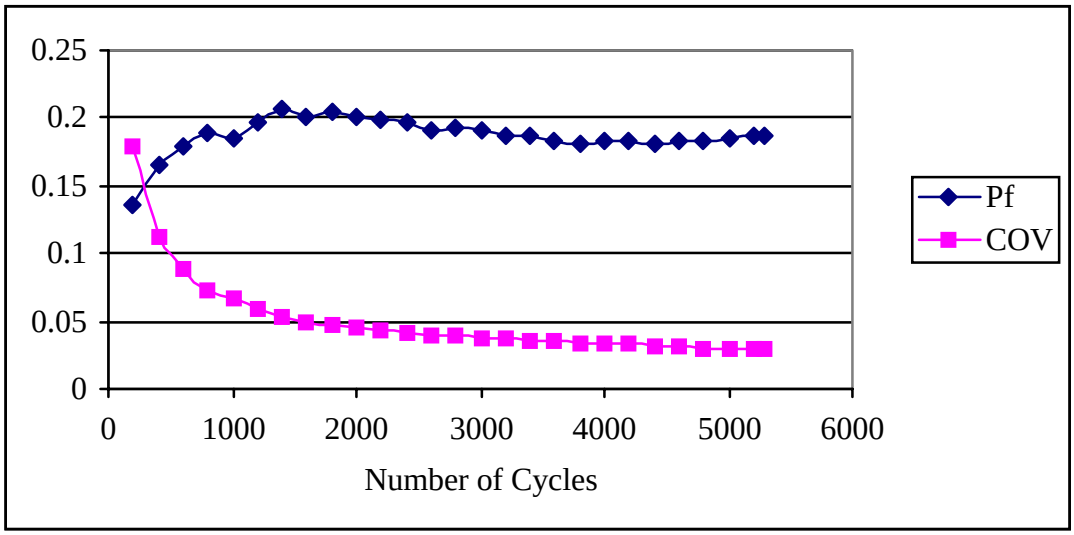

Figure 3.4 Results of Monte Carlo simulation for buckling reliability

Sensitivity Analysis

Deterministic Sensitivities of Limit State Function

The partial derivative of g with respect to each random variable gives a deterministic measure of its sensitivity to that variable. The relative importance of individual random variables is found by calculating the normalized sensitivities using the equation

$$\gamma_i = \left.\frac{\partial g}{\partial X_i'}\right|_* x_i'^* \Bigg/ \sum_{i=1}^{n}\left(\left.\frac{\partial g}{\partial X_i'}\right|_* x_i'^*\right) \tag{3.8}$$

and then normalizing the values with respect to one having the largest magnitude. The deterministic and normalized sensitivities at MPP for the $[\pm 45/90_4/\mp 45]_s$ specimen are given in Table 3.5 with the latter values also plotted in Fig. 3.5. The normalized sensitivities indicate that the applied load has the greatest influence on the limit state function, followed closely by E_{11} and cylinder diameter at a distant third. The effect of applied load is evident from the limit-state function formulation; however, the effects of E_{11} and cylinder diameter were not intuitively obvious prior to this analysis. The effect of individual ply thickness is also seen to be more significant than the corresponding orientation angle.

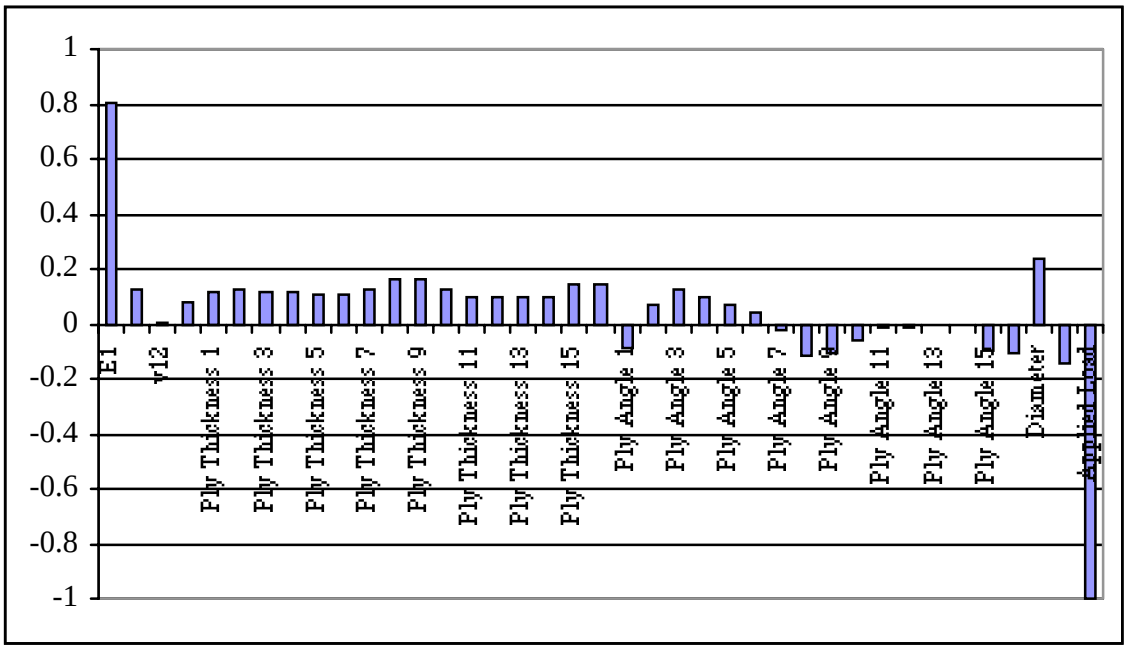

Figure 3.5 Normalized sensitivities

Table 3.5 Deterministic sensitivities of limit state function for specimen 4

Random Variable	$(\partial g / \partial X_i')_*$	γ_i	$(\gamma_i)_{\text{norm.}}$
E_{11}	6.7325E-03	4.5051E-01	7.9947E-01
E_{22}	1.3887E-02	7.0404E-02	1.2494E-01
ν_{12}	5.7268E+03	4.8772E-03	8.6550E-03
G_{12}	2.0828E-02	4.2489E-02	7.5400E-02
Ply Thickness 1	3.4174E+06	6.4401E-02	1.1429E-01
Ply Thickness 2	3.6443E+06	6.8676E-02	1.2187E-01
Ply Thickness 3	3.3224E+06	6.2610E-02	1.1111E-01
Ply Thickness 4	3.3929E+06	6.3939E-02	1.1346E-01
Ply Thickness 5	3.3511E+06	6.3152E-02	1.1207E-01
Ply Thickness 6	3.2515E+06	6.1274E-02	1.0874E-01
Ply Thickness 7	3.6541E+06	6.8861E-02	1.2220E-01
Ply Thickness 8	4.7967E+06	9.0388E-02	1.6040E-01
Ply Thickness 9	4.6600E+06	8.7811E-02	1.5583E-01
Ply Thickness 10	3.7226E+06	7.0151E-02	1.2449E-01
Ply Thickness 11	2.8606E+06	5.3910E-02	9.5667E-02
Ply Thickness 12	2.7974E+06	5.2719E-02	9.3553E-02
Ply Thickness 13	2.8313E+06	5.3358E-02	9.4688E-02
Ply Thickness 14	2.9109E+06	5.4857E-02	9.7348E-02
Ply Thickness 15	4.3647E+06	8.2248E-02	1.4596E-01
Ply Thickness 16	4.2379E+06	7.9859E-02	1.4172E-01
Ply Angle 1	-2.7543E+02	-4.6729E-02	-8.2925E-02
Ply Angle 2	-2.3055E+02	3.9105E-02	6.9394E-02
Ply Angle 3	2.0942E+02	7.1034E-02	1.2606E-01
Ply Angle 4	1.5349E+02	5.2066E-02	9.2394E-02
Ply Angle 5	1.0548E+02	3.5783E-02	6.3500E-02
Ply Angle 6	6.5501E+01	2.2222E-02	3.9434E-02
Ply Angle 7	8.9056E+01	-1.5108E-02	-2.6810E-02
Ply Angle 8	-3.7164E+02	-6.3055E-02	-1.1190E-01
Ply Angle 9	-3.6598E+02	-6.2096E-02	-1.1019E-01
Ply Angle 10	2.0173E+02	-3.4225E-02	-6.0735E-02
Ply Angle 11	-2.0116E+01	-6.8251E-03	-1.2112E-02
Ply Angle 12	-2.0665E+01	-7.0114E-03	-1.2442E-02
Ply Angle 13	-1.1853E+01	-4.0215E-03	-7.1365E-03
Ply Angle 14	-5.6443E-01	-1.9150E-04	-3.3982E-04
Ply Angle 15	3.2673E+02	-5.5435E-02	-9.8373E-02
Ply Angle 16	-3.5971E+02	-6.1032E-02	-1.0831E-01
Diameter	2.3608E+03	1.3344E-01	2.3680E-01
Length	-1.5325E+03	-8.0898E-02	-1.4356E-01
Applied Load, *P*	-1.0000E+00	-5.6351E-01	-1.0000E+00

Probabilistic Sensitivities of the Reliability Index

The probabilistic sensitivities of β with respect to the mean and standard deviation of individual random variables are found as

$$\frac{\partial \beta}{\partial \mu_{X_i}} = \frac{\left(\frac{\partial g}{\partial X_i'}\right)_*}{\sigma_{X_i}\sqrt{\sum_{i=1}^{39}\left(\frac{\partial g}{\partial X_i'}\right)_*^2}}, \quad i = 1, 2, ..., 39 \tag{3.9}$$

$$\frac{\partial \beta}{\partial \sigma_{X_i}} = \frac{\left(\frac{\partial g}{\partial X_i'}\right)_* x_i'^*}{\sigma_{X_i}\sqrt{\sum_{i=1}^{39}\left(\frac{\partial g}{\partial X_i'}\right)_*^2}}, \quad i = 1, 2, ..., 39 \tag{3.10}$$

The probabilistic sensitivities found from Eqs. (3.14) and (3.15) for $[\pm 45/90_4/\mp 45]_s$ specimen are shown in columns 2 and 4 of Table 3.6. The corresponding normalized probabilistic sensitivities, shown in columns 3 and 5 of Table 3.6, are calculated using the ratios

$$\delta_i = \frac{\partial \beta}{\partial \mu_{X_i}}\mu_{X_i} \Bigg/ \sum_{i=1}^{39}\left(\frac{\partial \beta}{\partial \mu_{X_i}}\mu_{X_i}\right), \qquad i = 1, 2, ..., 39 \tag{3.11}$$

$$\eta_i = \frac{\partial \beta}{\partial \sigma_{X_i}}\sigma_{X_i} \Bigg/ \sum_{i=1}^{39}\left(\frac{\partial \beta}{\partial \sigma_{X_i}}\sigma_{X_i}\right), \qquad i = 1, 2, ..., 39 \tag{3.12}$$

and dividing each ratio by the largest value in the group as

$$(\delta_i)_{norm} = \frac{\delta_i}{\delta_{\max}}; \quad \delta_{\max} = \max(|\delta_1|, |\delta_2|, \cdots, |\delta_{39}|) \tag{3.13}$$

$$(\eta_i)_{norm} = \frac{\eta_i}{\eta_{\max}}; \quad \eta_{\max} = \max(|\eta_1|, |\eta_2|, \cdots, |\eta_{39}|) \tag{3.14}$$

Table 3.6. Probabilistic sensitivities of the reliability index for specimen 4

Random Variable	$(\partial\beta / \partial\mu_{X_i})$	$(\delta_i)_{\text{norm}}$	$(\partial\beta / \partial\sigma_{X_i})$	$(\eta_i)_{\text{norm}}$
E_{11}	8.1380E-07	8.4340E-01	-3.5310E-07	2.8950E-01
E_{22}	1.6790E-06	1.3050E-01	-1.5050E-07	1.2360E-02
ν_{12}	6.9220E-01	9.0070E-03	-5.0290E-03	8.1130E-05
G_{12}	2.5170E-06	7.8710E-02	-1.6490E-07	6.5970E-03
Ply Thickness 1	4.1310E+02	1.1890E-01	-7.9250E+00	5.6570E-04
Ply Thickness 2	4.4050E+02	1.2680E-01	-9.0090E+00	6.4310E-04
Ply Thickness 3	4.0160E+02	1.1560E-01	-7.4870E+00	5.3450E-04
Ply Thickness 4	4.1010E+02	1.1810E-01	-7.8100E+00	5.5760E-04
Ply Thickness 5	4.0500E+02	1.1660E-01	-7.6200E+00	5.4400E-04
Ply Thickness 6	3.9300E+02	1.1310E-01	-7.1740E+00	5.1210E-04
Ply Thickness 7	4.4170E+02	1.2720E-01	-9.0580E+00	6.4660E-04
Ply Thickness 8	5.7980E+02	1.6690E-01	-1.5610E+01	1.1140E-03
Ply Thickness 9	5.6320E+02	1.6220E-01	-1.4730E+01	1.0520E-03
Ply Thickness 10	4.4990E+02	1.2950E-01	-9.4030E+00	6.7130E-04
Ply Thickness 11	3.4580E+02	9.9540E-02	-5.5510E+00	3.9630E-04
Ply Thickness 12	3.3810E+02	9.7340E-02	-5.3090E+00	3.7900E-04
Ply Thickness 13	3.4220E+02	9.8520E-02	-5.4370E+00	3.8820E-04
Ply Thickness 14	3.5180E+02	1.0130E-01	-5.7470E+00	4.1030E-04
Ply Thickness 15	5.2760E+02	1.5190E-01	-1.2930E+01	9.2280E-04
Ply Thickness 16	5.1220E+02	1.4750E-01	-1.2180E+01	8.6980E-04
Ply Angle 1	-3.3290E-02	-8.6260E-02	-4.6310E-04	2.9760E-04
Ply Angle 2	-2.7870E-02	7.2200E-02	-3.2460E-04	2.0850E-04
Ply Angle 3	2.5310E-02	1.3120E-01	-5.3560E-04	6.8820E-04
Ply Angle 4	1.8550E-02	9.6140E-02	-2.8760E-04	3.6960E-04
Ply Angle 5	1.2750E-02	6.6070E-02	-1.3590E-04	1.7460E-04
Ply Angle 6	7.9170E-03	4.1030E-02	-5.2420E-05	6.7360E-05
Ply Angle 7	1.0760E-02	-2.7890E-02	-4.8450E-05	3.1130E-05
Ply Angle 8	-4.4920E-02	-1.1640E-01	-8.4340E-04	5.4190E-04
Ply Angle 9	-4.4240E-02	-1.1460E-01	-8.1790E-04	5.2550E-04
Ply Angle 10	2.4380E-02	-6.3180E-02	-2.4850E-04	1.5960E-04
Ply Angle 11	-2.4310E-03	-1.2600E-02	-4.9470E-06	6.3570E-06
Ply Angle 12	-2.4980E-03	-1.2940E-02	-5.2090E-06	6.6940E-06
Ply Angle 13	-1.4330E-03	-7.4240E-03	-1.7120E-06	2.2010E-06
Ply Angle 14	-6.8220E-05	-3.5350E-04	-4.0480E-09	5.2020E-09
Ply Angle 15	3.9490E-02	-1.0230E-01	-6.5180E-04	4.1880E-04
Ply Angle 16	-4.3480E-02	-1.1270E-01	-7.9020E-04	5.0770E-04
Diameter	2.8530E-01	2.4640E-01	-1.1340E-02	2.4290E-03
Length	-1.8520E-01	-1.4930E-01	-4.4620E-03	8.9190E-04
Applied Load, *P*	-1.2090E-04	-1.0000E+00	-9.7480E-05	1.0000E+00

The plot of normalized probabilistic sensitivities with respect to the mean value of individual random variables is shown in Fig. 3.6. These sensitivities reconfirm, to some extent, the deterministic sensitivity results in that the mean values of the applied load and E_{11} are found to have a much stronger influence on the reliability index than those of other random variables. The influence of mean cylinder diameter is found to be less significant as was also indicated by deterministic sensitivities of the limit state function in Fig. 3.5. Besides these top three random variables (P, E_{11}, and D), the mean ply thicknesses are in the second category in terms of influence on β. However, if the effect of total as opposed to individual ply thicknesses is examined, a much greater sensitivity would be observed.

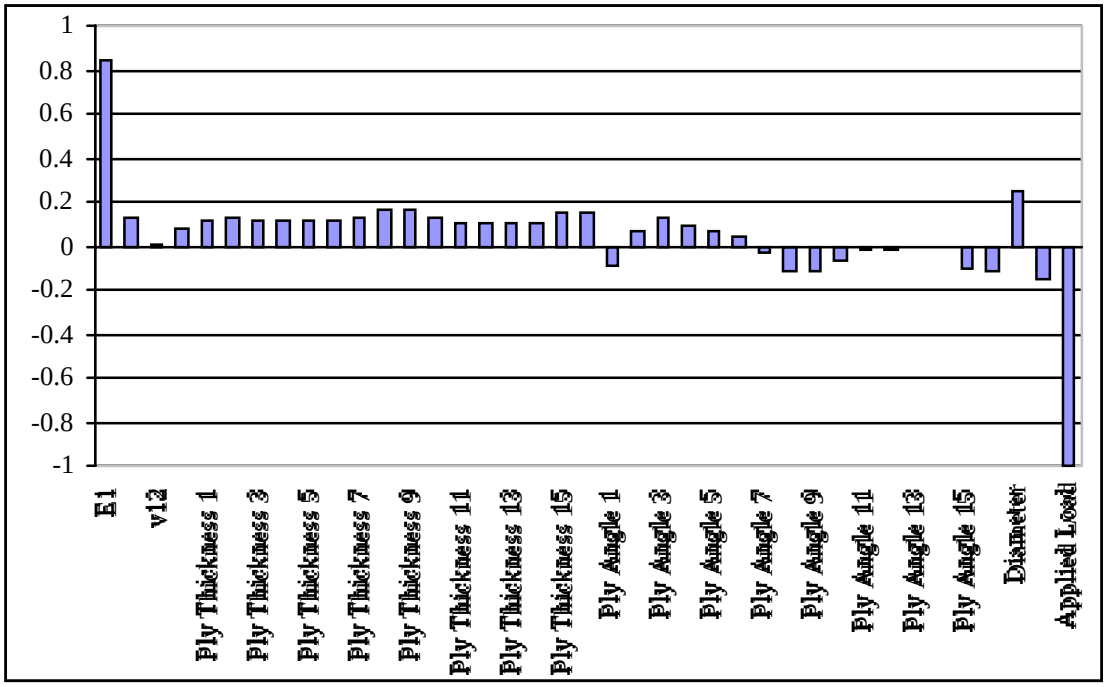

Figure 3.6 Normalized probabilistic sensitivities of β with respect to the mean value of each random variable

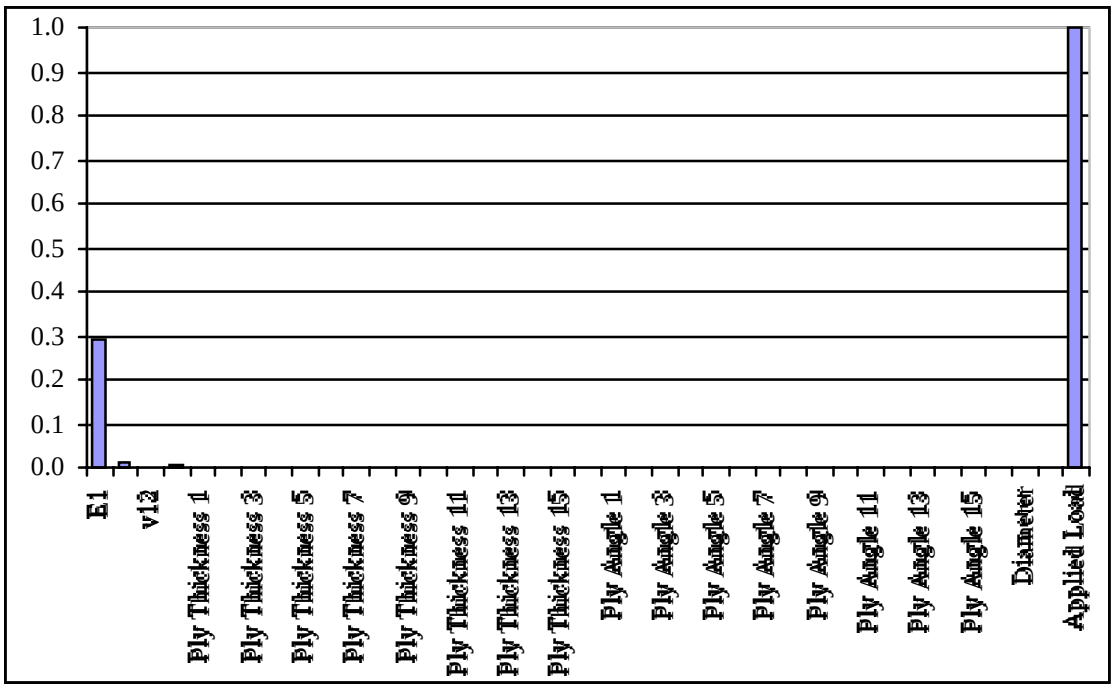

Figure 3.7 Normalized probabilistic sensitivities of β with respect to the standard deviation of each random variable

The plot of normalized probabilistic sensitivities with respect to the standard deviation of each random variable is shown in Fig. 3.7. The plot indicates that β is significantly more sensitive to uncertainty in P and E_{11} than the other 37 random variables.

Effects of Distribution Type and COV of the Applied Load on β

Since the results of reliability analysis indicate a large sensitivity to the applied load, the effects of the distribution type and coefficient of variation of P on β were also examined. Two different distribution types (Normal and Lognormal) and three different

values for coefficient of variation of *P* were considered. In both cases, the applied load was assumed to have a mean of 143,690 lb. The critical buckling load was determined from the algebraic response surface model and was not affected by the variance in applied load.

The results shown in Table 3.7 indicate that the coefficient of variation has a significant influence on β whereas the effect of the distribution type is relatively insignificant. It must be noted that in both cases the remaining 38 random variables were assumed to have normal distribution. This fact is important in the case of Monte Carlo simulation, but irrelevant in the case of Hasofer-Lind reliability index calculation. The reason the values of β associated with the two distribution types are not exactly identical is because in the lognormal case, the data is not dispersed symmetrically about the mean, as it is in the normal case.

Table 3.7 The effects of distribution and coefficient of variation of *P*

		Hasofer-Lind		Monte Carlo Simulation
P Distribution	COV (%)	β	P_f	P_f
Normal	1	1.7315	.042	.050
	5	0.9099	.181	.186
	10	0.5038	.309	.308
Lognormal	1	1.7326	.042	.050
	5	0.9188	.179	.184
	10	0.5421	.295	.295

Results of Specimens 1, 2 and 3

A sensitivity analysis was conducted for specimens 1, 2 and 3. Their distribution types, mean values and coefficients of variations of random variables are specified in Table 3.4. The ply pattern specified, as indicated previously in Table 3.3, are as follows:

Specimen 1: $[\pm 45/\mp 45]_{2s}$

Specimen 2: $[\pm 45/0/90]_{2s}$

Specimen 3: $[\pm 45/0_4/\mp 45]_s$

The deterministic sensitivity derivatives are shown in Table 3.8 while those for the probabilistic approach are shown in Table 3.9.

Table 3.8 Deterministic sensitivities of limit state function for specimen 1, 2 and 3

Random Variable	$(\gamma_i)_{\text{norm.}}$		
	Specimen 1	Specimen 2	Specimen 3
E_{11}	5.3177E-01	8.3212E-01	7.3822E-01
E_{22}	6.5451E-02	6.4709E-02	1.4473E-01
ν_{12}	1.3888E-02	5.1279E-03	9.3684E-03
G_{12}	4.8625E-01	7.3314E-02	1.0011E-01
Ply Thickness 1	1.1169E-01	1.2143E-01	4.2650E-02
Ply Thickness 2	1.0578E-01	1.5171E-01	4.5929E-02
Ply Thickness 3	1.1326E-01	1.0317E-01	1.4124E-01
Ply Thickness 4	1.1694E-01	1.0201E-01	1.4299E-01
Ply Thickness 5	1.2285E-01	9.1156E-02	1.4104E-01
Ply Thickness 6	1.2575E-01	9.7654E-02	1.4208E-01
Ply Thickness 7	1.1672E-01	1.2081E-01	1.3274E-01
Ply Thickness 8	1.3075E-01	1.3460E-01	1.5041E-01
Ply Thickness 9	1.2058E-01	1.3509E-01	1.4489E-01
Ply Thickness 10	1.2552E-01	1.2115E-01	1.3291E-01
Ply Thickness 11	1.2386E-01	1.0365E-01	9.1386E-02
Ply Thickness 12	1.1950E-01	1.3077E-01	9.4767E-02
Ply Thickness 13	1.2939E-01	1.2552E-01	8.8619E-02
Ply Thickness 14	1.3443E-01	1.1060E-01	9.1501E-02
Ply Thickness 15	1.2047E-01	1.0515E-01	1.5087E-01
Ply Thickness 16	1.1183E-01	1.1256E-01	1.4216E-01
Ply Angle 1	-3.3156E-01	1.1028E-02	4.0752E-02
Ply Angle 2	-2.6414E-01	-5.8536E-02	-2.4857E-02
Ply Angle 3	-1.9408E-01	-8.6896E-06	9.8673E-07
Ply Angle 4	-1.2057E-01	-3.2414E-02	7.0570E-07
Ply Angle 5	-6.4461E-02	-4.3119E-02	3.2963E-07
Ply Angle 6	-1.3488E-02	-7.1985E-07	1.6328E-07
Ply Angle 7	3.4386E-02	2.3961E-04	9.6772E-02
Ply Angle 8	7.3834E-02	2.0462E-02	1.3748E-01
Ply Angle 9	1.1022E-01	2.3762E-02	1.4217E-01
Ply Angle 10	1.3918E-01	6.1652E-03	1.2562E-01
Ply Angle 11	1.6028E-01	-1.3151E-06	9.9413E-11
Ply Angle 12	1.7688E-01	-3.9031E-02	1.1514E-09
Ply Angle 13	1.8826E-01	-2.8110E-02	3.2642E-12
Ply Angle 14	1.9029E-01	-2.1580E-07	1.3610E-09
Ply Angle 15	1.9032E-01	1.8791E-03	1.0796E-01
Ply Angle 16	1.8347E-01	4.5697E-04	8.9776E-02
Diameter	-1.8647E-01	3.7199E-02	-6.0124E-02
Length	3.9204E-01	7.5305E-02	1.6076E-01
Applied Load, *P*	-1.0000E+00	-1.0000E+00	-1.0000E+00

Table 3.9 Probabilistic sensitivities of the reliability index for specimen 1,2 and 3

Random Variable	$(\delta_i)_{\text{norm}}$			$(\eta_i)_{\text{norm}}$		
	Specimen 1	Specimen 2	Specimen 3	Specimen 1	Specimen 2	Specimen 3
E_{11}	3.26E-01	9.8520E-01	7.0538E-01	4.3327E-02	3.9508E-01	2.0253E-01
E_{22}	4.16E-02	7.3266E-02	1.3919E-01	1.2570E-03	3.8966E-03	1.4063E-02
ν_{12}	8.90E-03	5.7717E-03	9.0385E-03	7.9153E-05	3.3313E-05	8.1700E-05
G_{12}	2.82E-01	8.3382E-02	9.6267E-02	8.4806E-02	7.4046E-03	9.8701E-03
Ply Thickness 1	7.17E-02	1.3667E-01	4.1158E-02	2.0568E-04	7.4716E-04	6.7747E-05
Ply Thickness 2	6.79E-02	1.7078E-01	4.4323E-02	1.8447E-04	1.1666E-03	7.8631E-05
Ply Thickness 3	7.27E-02	1.1611E-01	1.3629E-01	2.1149E-04	5.3923E-04	7.4279E-04
Ply Thickness 4	7.51E-02	1.1480E-01	1.3797E-01	2.2542E-04	5.2713E-04	7.6155E-04
Ply Thickness 5	7.89E-02	1.0258E-01	1.3609E-01	2.4873E-04	4.2086E-04	7.4101E-04
Ply Thickness 6	8.07E-02	1.0990E-01	1.3709E-01	2.6063E-04	4.8305E-04	7.5193E-04
Ply Thickness 7	7.49E-02	1.3597E-01	1.2808E-01	2.2460E-04	7.3946E-04	6.5603E-04
Ply Thickness 8	8.39E-02	1.5150E-01	1.4513E-01	2.8171E-04	9.1806E-04	8.4246E-04
Ply Thickness 9	7.74E-02	1.5205E-01	1.3980E-01	2.3965E-04	9.2480E-04	7.8171E-04
Ply Thickness 10	8.06E-02	1.3635E-01	1.2825E-01	2.5969E-04	7.4368E-04	6.5793E-04
Ply Thickness 11	7.95E-02	1.1664E-01	8.8185E-02	2.5285E-04	5.4423E-04	3.1101E-04
Ply Thickness 12	7.67E-02	1.4719E-01	9.1447E-02	2.3540E-04	8.6655E-04	3.3447E-04
Ply Thickness 13	8.31E-02	1.4128E-01	8.5515E-02	2.7594E-04	7.9841E-04	2.9247E-04
Ply Thickness 14	8.63E-02	1.2447E-01	8.8296E-02	2.9780E-04	6.1972E-04	3.1187E-04
Ply Thickness 15	7.73E-02	1.1834E-01	1.4557E-01	2.3924E-04	5.6017E-04	8.4777E-04
Ply Thickness 16	7.18E-02	1.2668E-01	1.3717E-01	2.0617E-04	6.4196E-04	7.5274E-04
Ply Angle 1	-2.14E-01	1.2404E-02	3.9328E-02	1.8272E-03	6.1541E-06	6.1882E-05
Ply Angle 2	-1.70E-01	-6.5816E-02	-2.3990E-02	1.1582E-03	1.7328E-04	2.3010E-05
Ply Angle 3	-1.25E-01	0.0000E+00	0.0000E+00	6.2449E-04	7.8354E-05	2.7278E-05
Ply Angle 4	-7.76E-02	-3.6450E-02	0.0000E+00	2.4066E-04	5.3136E-05	1.9509E-05
Ply Angle 5	-4.15E-02	-4.8486E-02	0.0000E+00	6.8722E-05	9.4044E-05	9.1126E-06
Ply Angle 6	-8.67E-03	0.0000E+00	0.0000E+00	3.0066E-06	6.4909E-06	4.5138E-06
Ply Angle 7	2.21E-02	2.6949E-04	9.3382E-02	1.9520E-05	2.9304E-09	3.4875E-04
Ply Angle 8	4.74E-02	2.3017E-02	1.3265E-01	8.9930E-05	2.1195E-05	7.0383E-04
Ply Angle 9	7.08E-02	2.6730E-02	1.3718E-01	2.0029E-04	2.8575E-05	7.5282E-04
Ply Angle 10	8.93E-02	6.9345E-03	1.2122E-01	3.1917E-04	1.9228E-06	5.8780E-04
Ply Angle 11	1.03E-01	0.0000E+00	0.0000E+00	4.2311E-04	1.1859E-05	2.7482E-09
Ply Angle 12	1.13E-01	-4.3890E-02	0.0000E+00	5.1521E-04	7.7046E-05	3.1829E-08
Ply Angle 13	1.21E-01	-3.1611E-02	0.0000E+00	5.8347E-04	3.9980E-05	9.0238E-11
Ply Angle 14	1.22E-01	0.0000E+00	0.0000E+00	5.9612E-04	1.9459E-06	3.7623E-08
Ply Angle 15	1.22E-01	2.1135E-03	1.0418E-01	5.9626E-04	1.7811E-07	4.3409E-04
Ply Angle 16	1.18E-01	5.1397E-04	8.6632E-02	5.5422E-04	1.0479E-08	3.0019E-04
Diameter	-1.20E-01	4.1848E-02	-5.8030E-02	5.7638E-04	7.0049E-05	1.3475E-04
Length	2.51E-01	8.4734E-02	1.5511E-01	2.5209E-03	2.8718E-04	9.6247E-04
Applied Load, *P*	-1.00E+00	-1.0000E+00	-1.0000E+00	1.0000E+00	1.0000E+00	1.0000E+00

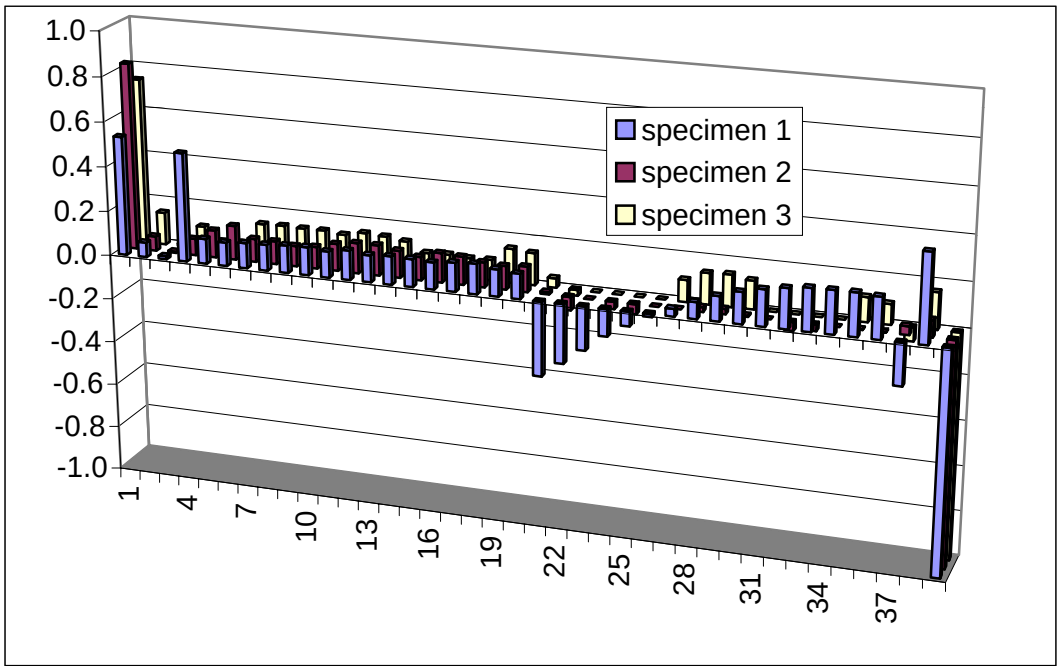

Figure 3.8 Deterministic sensitivities $(\gamma_i)_{norm}$ of specimen 1, 2 and 3

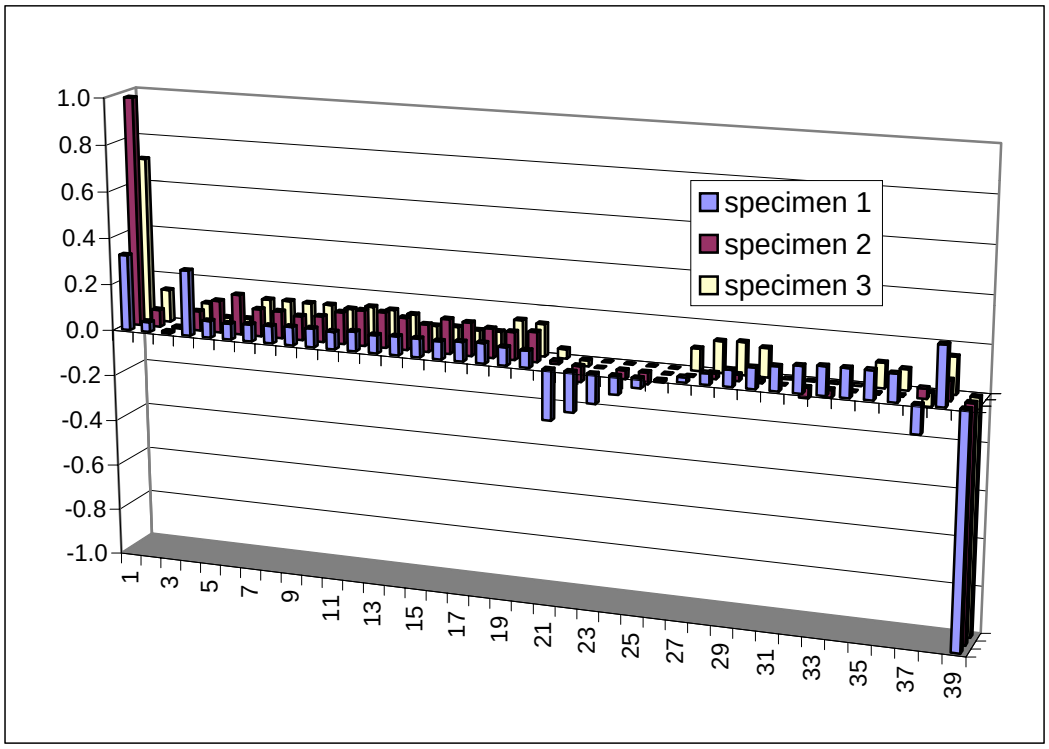

Figure 3.9 Normalized probabilistic sensitivities of β with respect to the mean value of each random variable for specimen 1, 2 and 3

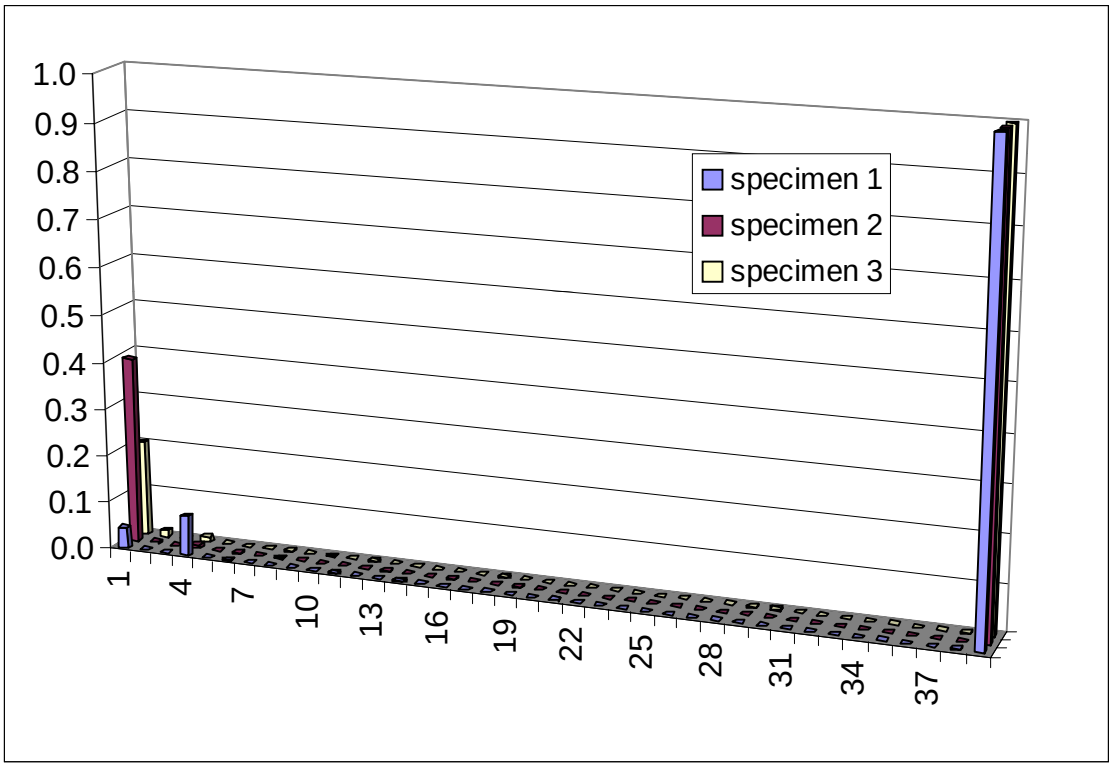

Figure 3.10 Normalized probabilistic sensitivities of β with respect to the standard deviation of each random variable for specimen 1, 2 and 3

For the deterministic sensitivities, P and E_{11} have the biggest influence in all 3 specimens. G_{12} also has a relatively big influence in specimen 1. For the probabilistic sensitivities of β with respect to the mean values of each variable, the applied load and E_{11} still have the biggest influence in all 3 specimens. For normalized probabilistic sensitivities of β with respect to the standard deviation of each random variable, the applied load and E_{11} have stronger influence than other variables in specimens 2 and 3, while the applied load and G_{12} have the strongest influence in specimen 1. With some exceptions, the reliability of these specimens, as judged by the normalized sensitivity derivatives, is still most sensitive to the applied load P and Young's Modulus E_{11}.

Chapter IV

RELIABILITY-BASED OPTIMIZATION OF COMPOSITE CYLINDRICAL SHELLS UNDER AXIAL COMPRESSION

Introduction

This chapter discusses the reliability-based optimization of laminated circular cylinders under axial compression. Structural reliability is measured in terms of Hasofer-Lind reliability index, as discussed in Chapter 3.

The optimization analysis is based on the response surface approximation of axial buckling force, $\tilde{P}_{cr}$. In generating the response surface model, two different techniques are considered. In the first technique, a Monte Carlo simulation is conducted to find a nonlinear model that provides a fairly accurate estimate of buckling load at any design point over a wide range of values for individual random variables (including the design variables). This approach requires a relatively large number of Monte Carlo simulations in order to accurately capture the effect of variation in each variable on the buckling load. This is referred to as the global response surface technique.

In the second technique, a locally accurate response surface model is constructed based on the $n+1$ point integration technique where n is the number of random variables being considered. This technique is used to generate a new response surface model for each design search iteration cycle focused on a small subregion of design space.

Global Response Surface Technique

A single global response surface model for axial buckling force is generated as a function of all material and geometric random variables. The term global implies validity over the entire design domain confined by bounds imposed on individual random variables. For a 16-ply symmetric laminate, there are 22 random variables to be included in the response surface equation. The list of these random variables in shown in Table 4.1.

Because of the nonlinear relationship between the buckling load and most of the random variables and the need for the model to be accurate over the entire design domain, a fully quadratic response surface model needs to be generated. A full quadratic equation with all higher order terms present result in 276 unknown coefficients. In its generic form, this equation can be written as

$$\tilde{P}_{cr} = a_0 + \sum_{i=1}^{22} b_i X_i + \sum_{i=1}^{22} c_i X_i^2 + \sum_{i=1}^{21} \sum_{j=i+1}^{22} d_i X_i X_j \tag{4.1}$$

To obtain an accurate (i.e., very good) estimate of the unknown coefficients, 3,000 Monte Carlo simulation cycles were conducted. Each random variable in this simulation was assumed to have a uniform distribution with the lower and upper bounds calculated according to the relations

$$\begin{aligned} X_i^l &= (1-\varsigma)\mu_{X_i} \\ X_i^u &= (1+\varsigma)\mu_{X_i} \end{aligned} \tag{4.2}$$

The values of mean and incremental change in each random variable is shown in Table 4.1.

Table 4.1 Mean values and bound increments used in Monte Carlo simulation

Random Variable	μ_{X_i}	ς(%)
E_{11}, psi	1.8E7	4
E_{22}, psi	1.35E6	5
ν_{22}	.226	6
G_{12}, psi	5.43E6	7
t_{ply}, in	.005	50
θ_1, deg.	45	26
θ_2, deg.	-45	26
θ_3, deg.	90	26
θ_4, deg.	90	26
θ_5, deg.	90	26
θ_6, deg.	90	26
θ_7, deg.	-45	26
θ_8, deg.	45	26
Diameter, in	15	50
Length, in	14	50

For each random variable, we can obtain the uniformly distributed X_i by

$$X_i = X_i^l + (X_i^u - X_i^l)r \tag{4.3}$$

where r is a uniformly distributed number with $0 \le r < 1$.

We used the response surface analysis procedure in SAS software for calculating the unknown coefficients in the response surface equation.

Before using the response surface equation in the optimization analysis, it was checked for accuracy. The mean buckling load is found to be 144,218 lb with a coefficient of determination R^2= 0.9774, coefficient of variation of 3.04%, and a root mean square error (RMSE) of 4,383.26. Because of the range of values of each random variable in the Monte Carlo simulation, we are able to generate and use a single response surface model which is valid for all three combinations of cylinder length and diameter.

In spite of high R^2 and small RMSE, the buckling force predictions from the response surface model were compared with those found directly from the shell analysis code. The maximum difference in the buckling loads was found to be approximately 3%, which is almost equal to the COV of the response surface equation.

Weight Minimization

The weight minimization problem is formulated as

Min. $W(X_i)$, i =1,2,...,22

s.t.

$$\beta > \beta_{\min}$$

$$\mu_{X_j}^l < \mu_{X_j} < \mu_{X_j}^u, \; j = 1,2,..., \text{NDV}$$

where $(\mu_{X_1}, \mu_{X_2}, \cdots, \mu_{X_{NDV}})$ represent the mean values of a subset of random variables treated as design variables. Since the cylinder is made of a constant density material and the specific weight was not treated as a random variable in our analysis, we decided to use the material volume as a surrogate for weight.

In optimizing the cylinder, the mean thickness of individual plies were considered as the design variables with the corresponding standard deviations fixed. The shell laminate is assumed to be symmetric, which requires only the thickness of plies on one side of the plane of symmetry to be treated as design variables. The material properties and ply orientation angles were treated as random variables with specific means and standard deviations. The cylinder length and diameter were allowed to have three specific mean values.

To perform the design optimization studies, the reliability analysis code was coupled with the DOT[30] optimization program where the response surface model was used to obtain the buckling response. The optimization solutions are based on the method of sequential quadratic programming. The lower and upper bounds on ply thickness are chosen to be 0.0026 in. and 0.007 in. , respectively.

We examined three different values for β_{min} (i.e., 3.09, 3.72, and 4.26). The β values and their corresponding reliability are shown in Table 4.2. The optimization results are shown in Table 4.3. The values of the mean axial and mean buckling loads are also shown in Table 4.3.

Table 4.2 β values and corresponding reliabilities

β	Reliability
3.09	0.999
3.72	0.9999
4.26	0.99999

Table 4.3 Optimization results for weight minimization

		Mean Values		
Design Exp.	Parameter[a]	$\beta_{\min} = 3.09$	$\beta_{\min} = 3.72$	$\beta_{\min} = 4.26$
1	P, lb	143690	143690	143690
	$\tilde{P}_{cr}$, lb	162631.018	166741.485	169817.556
	V, in^3	51.858	52.585	53.213
	t_1, in (45)	0.0066929	0.0069999	0.0067245
	t_2, in (-45)	0.0070000	0.0070000	0.0070000
	t_3, in (90)	0.0069976	0.0062224	0.0067173
	t_4, in (90)	0.0050790	0.0056137	0.0062750
	t_5, in (90)	0.0026000	0.0026000	0.0026004
	t_6, in (90)	0.0070000	0.0070000	0.0070000
	t_7, in (-45)	0.0026000	0.0026000	0.0026000
	t_8, in (45)	0.0031286	0.0036362	0.0032509
	D, in	20.0	20.0	20.0
	L, in	10.0	10.0	10.0
2	P, lb	143690	143690	143690
	$\tilde{P}_{cr}$, lb	161796.307	165441.246	168760.053
	V, in^3	58.448	59.251	59.940
	t_1, in (45)	0.0050275	0.0049061	0.0048684
	t_2, in (-45)	0.0055967	0.0055715	0.0056314
	t_3, in (90)	0.0031384	0.0030434	0.0031605
	t_4, in (90)	0.0049807	0.0052309	0.0055585
	t_5, in (90)	0.0026000	0.0026000	0.0026000
	t_6, in (90)	0.0064662	0.0070000	0.0070000
	t_7, in (-45)	0.0070000	0.0070000	0.0070000
	t_8, in (45)	0.0063088	0.0063282	0.0063427
	D, in	15.0	15.0	15.0
	L, in	15.0	15.0	15.0
3	P, lb	143690	143690	143690
	$\tilde{P}_{cr}$, lb	162085.471	165976.979	169573.945
	V, in^3	54.572	55.335	56.035
	t_1, in (45)	0.0056549	0.0056584	0.0058299
	t_2, in (-45)	0.0049778	0.0050325	0.0047818
	t_3, in (90)	0.0029505	0.0030163	0.0032725
	t_4, in (90)	0.0059979	0.0063456	0.0069087
	t_5, in (90)	0.0026000	0.0026000	0.0026000
	t_6, in (90)	0.0068751	0.0070000	0.0068083
	t_7, in (-45)	0.0070000	0.0070000	0.0070000
	t_8, in (45)	0.0070000	0.0070000	0.0069994
	D, in	10.0	10.0	10.0
	L, in	20.0	20.0	20.0

[a] Ply angles shown in parentheses

In design experiments 2 and 3, the thickness of middle plies (layers 6, 7 and 8) are near the upper bound, while the 5^{th} layer arrived close to the lower bounds. In design experiment 1, layers 1, 2 and 6 are near the upper bound, while layers 5 and 7 are close to the lower bound. It is observed that a substantial increase in reliability can be obtained with a minimal increase in wall thickness and material volume.

The variations in the optimum mean buckling load and cylinder volume are shown in Fig. 4.1. For all level of reliability index, the cylinder in design experiment 3 is seen to be stronger than those in the other two design experiments. Comparing the optimal design for design experiment 1 with that of 2, we see that even though the cylinder in design experiment 1 is lighter than that in 2, it has a slightly higher buckling load. The variations in length and diameter indicate that the shorter cylinder with larger diameter to be stronger than the longer cylinder with smaller diameter.

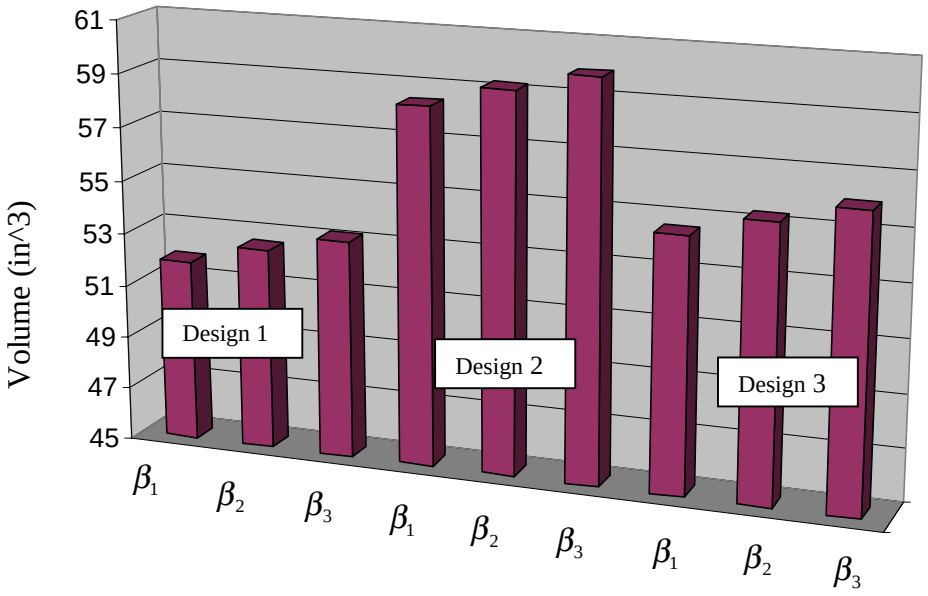

(a)

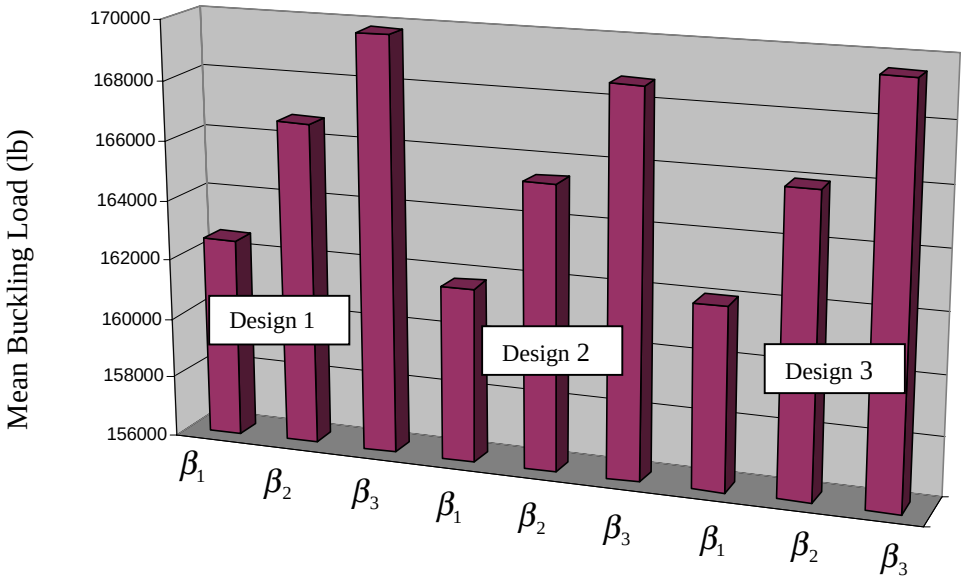

(b)

$\beta_1 = 3.09; \quad \beta_2 = 3.72; \quad \beta_3 = 4.26$

Figure 4.1 Variation of mean buckling load (a) and material volume (b) as a function of reliability index

Reliability Maximization

The reliability maximization problem is formulated as

Max. $\beta(X_i)$, i =1,2,...,22

s.t.

$$V \le V_{\max}$$

$$\mu_{X_j}^{l} < \mu_{X_j} < \mu_{X_j}^{u},\ j = 1,2,..., \text{NDV}$$

where V is the material volume of the cylinder. The results of this optimization are shown in Table 4.4. In each design experiment, the cylinder reliability is maximized based on two different limits on volume. This is done to examine the effect of volume constraint on reliability index.

From the results we see a several-cubic inch increase in volume results in a considerable increase in reliability index. The sensitivity of reliability index to volume is clearly evident in these results. It is interesting to note that in this optimization case design experiment 4 results in a lighter and stronger cylinder than the other two. By allowing the volume in design experiment 4 to increase to 52.5 in^3, the cylinder has a buckling load of 166,849 lb whereas design experiment 5 with a volume constraint of 58.5 in^3 resulted in a buckling load of 162,834 lb, and experiment 6 with a volume constraint of 58.5 in^3 resulted in a buckling load of only 162,077 lb.

Table 4.4 Optimization results for reliability maximization

Design Exp	Parameter	Mean Values	
		Low	High
4	β	3.803	6.326
	P, lb	143690	143690
	$\tilde{P}_{cr}$, lb	166848.990	184339.019
	V_{max}, in^3	52.5	55.5
	t_1, in (45)	0.0066983	0.0069649
	t_2, in (-45)	0.0070000	0.0070000
	t_3, in (90)	0.0060949	0.0070000
	t_4, in (90)	0.0062424	0.0070000
	t_5, in (90)	0.0026000	0.0026000
	t_6, in (90)	0.0070000	0.0070000
	t_7, in (-45)	0.0026000	0.0028334
	t_8, in (45)	0.0035065	0.0037972
	D, in	20.0	20.0
	L, in	10.0	10.0
5	β	3.280	6.864
	P, lb	143690	143690
	$\tilde{P}_{cr}$, lb	162834.180	185807.662
	V_{max}, in^3	58.5	63.0
	t_1, in (45)	0.0051650	0.0046351
	t_2, in (-45)	0.0054642	0.0062041
	t_3, in (90)	0.0029478	0.0038056
	t_4, in (90)	0.0052679	0.0069806
	t_5, in (90)	0.0026067	0.0026000
	t_6, in (90)	0.0066962	0.0069998
	t_7, in (-45)	0.0069944	0.0070000
	t_8, in (45)	0.0061512	0.0063579
	D, in	15.0	15.0
	L, in	15.0	15.0
6	β	3.103	6.578
	P, lb	143690	143690
	$\tilde{P}_{cr}$, lb	162077.777	185119.581
	V_{max}, in^3	54.5	59.0
	t_1, in (45)	0.0054847	0.0049459
	t_2, in (-45)	0.0049751	0.0050188
	t_3, in (90)	0.0030721	0.0061180
	t_4, in (90)	0.0059383	0.0069813
	t_5, in (90)	0.0026000	0.0026113
	t_6, in (90)	0.0070000	0.0069713
	t_7, in (-45)	0.0070000	0.0069995
	t_8, in (45)	0.0070000	0.0070000
	D, in	10.0	10.0
	L, in	20.0	20.0

Local Response Surface Technique

In the previous section, the application of a single global response surface equation for buckling load estimation in both reliability analysis and design optimization was described. Although that technique resulted in a substantial computational savings over the use of exact analysis at every iteration, it still required 3000 Monte Carlo simulation cycles for development of an accurate response surface model. The technique explored in this section seeks to reduce that computational burden even further with minimal loss of accuracy in the optimization results.

The procedure works as follows. Instead of using a single nonlinear global response model that is valid over the entire design space, a series of linear response surface models was used with each being accurate over a localized region of the design space. During each optimization cycle, the search for a better design is limited to the region where the local response surface model is valid. At the completion of each optimization cycle, a new response model is generated for use in the next optimization cycle. The procedure is repeated until the objective function converges. Figure 4.2 illustrates the search technique over a simple two-dimensional space. The arrow in each block indicates the initial and final points within each local optimization.

The computational efficiency of this technique is due to its requirement for much fewer Monte Carlo simulation cycles. The local response models are generated based on the $n+1$ point integration simulations, where n is the number of random variables present in the response surface model. Since we are using response observations for only $n+1$ experiments, we can only generate a linear response surface model. This limitation should not pose a problem as each model is used over a small sub-region of the design

space. The selection of random value for each variable is based on the procedure described in Appendix C.

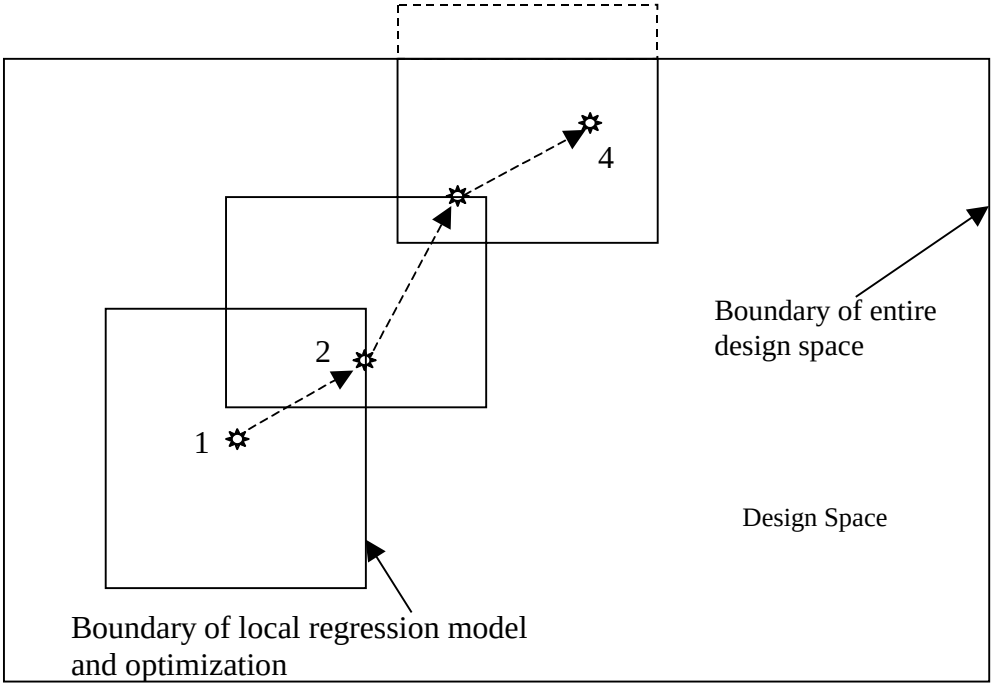

Figure 4.2 Illustration of optimization based on multiple local regression models

The optimization scheme based on the sequential application of local response models is described by the flowchart in Fig. 4.3.

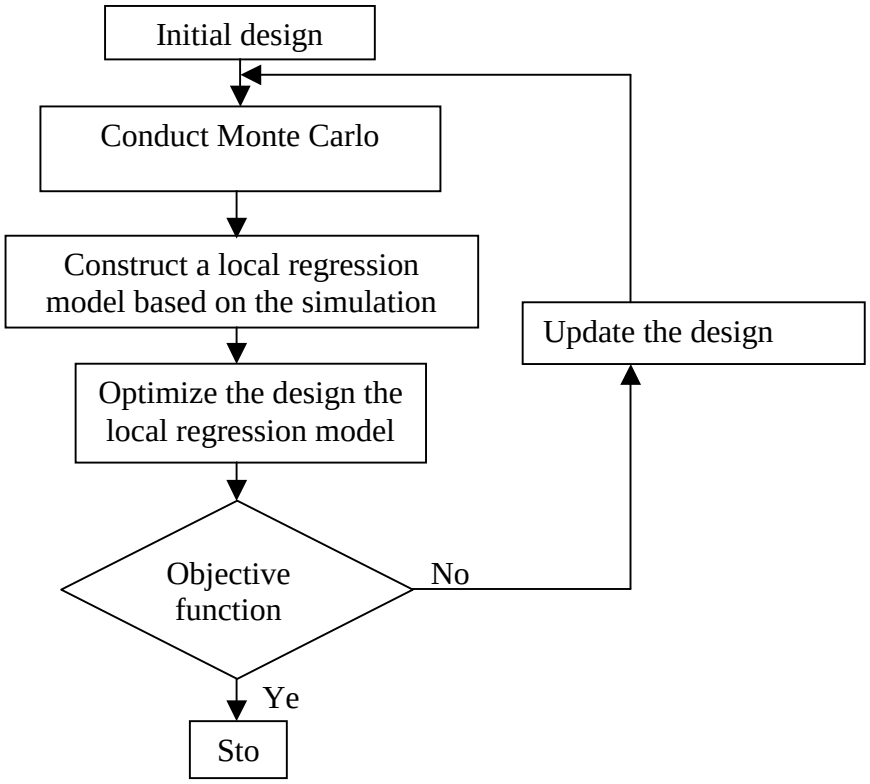

Figure 4.3 Flow chart of optimization based on multiple local regression models

The optimization results based on this technique are listed in Table 4.5 and Figure 4.4.

Table 4.5 Multiple local optimization results for weight minimization with reliability constraint of $\beta_{\min} = 3.09$

Case	Global RS technique			Local RS technique			Difference in answer (%)	Difference in CPU time (hr)
	Initial	Final	CPU time (hr)	Initial	Final	CPU time		
1	56.85	55.04	350	56.85	56.62	16	2.8	334
2	56.85	59.74	350	56.85	58.83	16	1.54	334
3	56.85	55.80	350	34.03	55.41	19	0.7	331
4	56.85	55.80	350	83.20	55.08	19	1.3	331
5	56.85	58.45	350	34.03	57.73	21	1.2	329
6	56.85	58.45	350	83.20	57.60	19	1.5	331

Case 1: All COV=1% except $COV_P = 3.04\%$

Case 2: $COV_{E_{11}} = 3.19\%$, $COV_{E_{22}} = 4.26\%$, $COV_v = 5\%$, $COV_{G_{12}} = 5.16\%$, $COV_P = 3.04$, $COV_t = 5\%$ and all other COV = 1%

Case 3, 4: All COV=1%

Case 5, 6: $COV_{E_{11}} = 3.19\%$, $COV_{E_{22}} = 4.26\%$, $COV_v = 5\%$, $COV_{G_{12}} = 5.16\%$, $COV_P = 3.04$ and all other COV = 1%

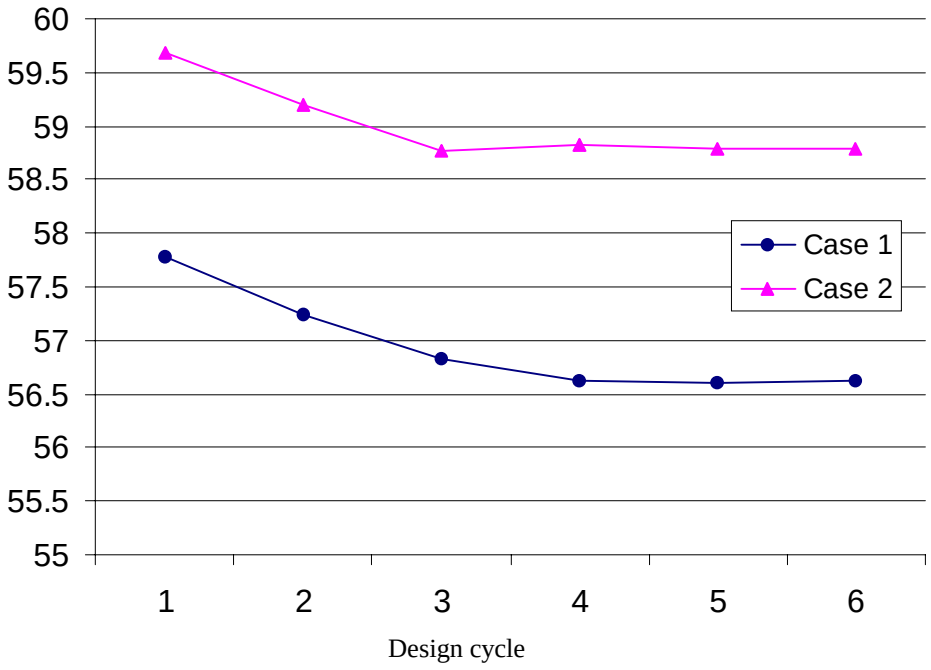

(a)

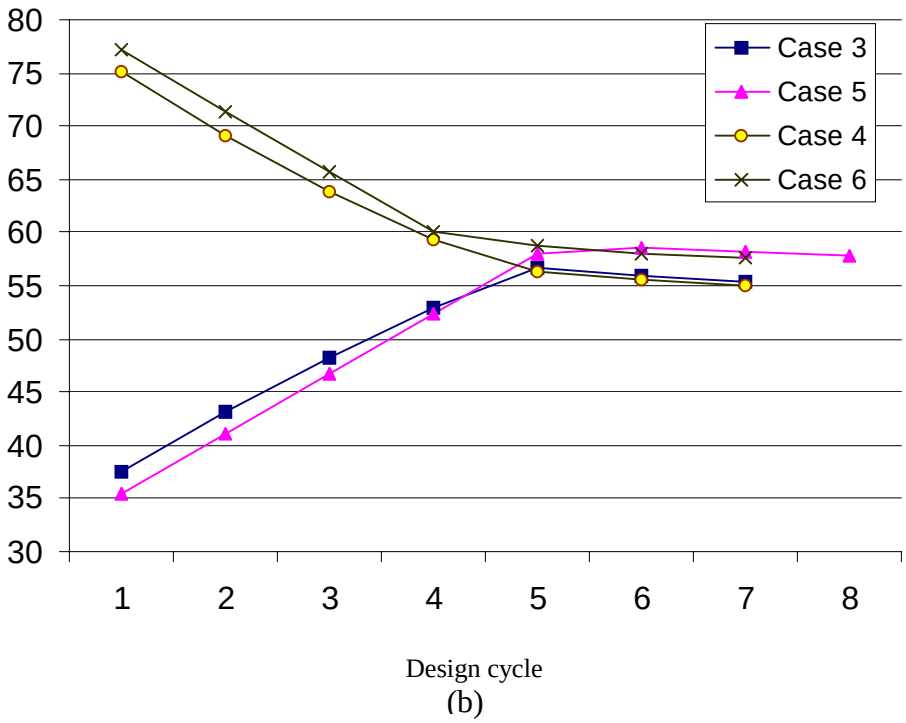

(b)

Figure 4.4 Optimization Convergence History

The optimization generated from global response model optimization technique and multiple local response models technique have little difference, while the latter takes much less time. Thus apparently the multiple local response models technique is more efficient than the global model technique.

The plots also show the effect of the coefficient of variation on the optimization results. When the random variables have larger coefficients of variations, which increase the probability of structure failure, the ply thicknesses tend to increase in order to maintain the minimum reliability constraint, thus resulting the increase in shell volume. This trend can be seen in Figure 4.3, in which Case 2, Case 5 and Case 6 have larger COV's than Case 1, Case 3 and Case 4, respectively.

The optimization was started with the initial values of the design variables being at the lower bounds in Case 3 and Case 5, and at the upper bounds in Case 4 and Case 6. Figure 4.3(b) shows that the same objective function values are reached no matter where the optimization was begun.

Chapter V

SUMMARY AND CONCLUSIONS

Reliability Analysis of Anisotropic Circular Cylinders

The reliability of anisotropic circular cylinders with axial buckling as the mode of failure was investigated. A large number of Monte Carlo simulations cycles were performed and the RSREG procedure of statistics software SAS was used to construct the full quadratic response surface model for estimation of axial buckling force. The response surface equation was used for calculation of component reliability measured in terms of Hasofer-Lind reliability index. The probability of failure was also calculated using the Monte Carlo simulation method, which is shown to be very close to that from the Hasofer-Lind reliability index.

The response surface model was also used to investigate sensitivity. The deterministic sensitivity derivatives of the limit state function, defining the surface separating the safe from the failure region, with respect to material properties, geometric parameters, and applied load were studied. For the four anisotropic cylinders, ply pattern, applied load, Young's modulus E_{11}, and cylinder diameter, were found to have the greatest influence on the limit state function. The probabilistic sensitivities of the reliability index β with respect to the mean and standard deviation of material

properties, geometric parameters, and applied load were calculated. These results also indicate Young's modulus E_{11} and diameter have the greatest influence on reliability index β. For the cylinder made only of ± 45 plies, G_{12} is also seen to have a large influence on β. Although the influence of each ply thickness was found to be small, the effect of total thickness on buckling load is large, as expected.

As for the influence of distribution type and coefficient of variation of applied load on reliability index β, it was found that the distribution type has little effect on β while the influence of coefficient of variation is more significant. The probability of failure increases as the coefficient of variation is increased.

Reliability-Based Optimization of Anisotropic Circular Cylinders

Two design optimization cases were investigated. In the first case, the cylinder weight is minimized subject to a reliability constraint; in the second case, the cylinder reliability is maximized subject to a weight/volume constraint. In both cases three different combinations of cylinder diameter and length were examined. The mean thickness of each ply in one side of a symmetric laminate was treated as a design variable for a total of eight variables. For the weight minimization problem, three different limits for reliability index were considered. Results showed that for cylinders with different diameters and lengths, the optimum thickness of each layer varies. It was observed that a small increase in wall thickness and material volume could result in a substantial increase in reliability index. For the reliability maximization problem, two different limits on

maximum material volume were examined. The results also showed that a small increase in material volume could lead to a big increase in reliability.

The optimization technique based on a single global nonlinear response surface model of axial buckling force was compared with one based on sequential application of local response surface models. Development of a globally accurate model required the use of a full quadratic equation, which required 3000 Monte Carlo simulation cycles for accurate estimation of its unknown coefficients. In contrast, each linear response model in the local response surface technique required 23 Monte Carlo simulation cycles for a total of approximately 160 simulations. The weight minimization problem was repeated. The results from global and local response surface techniques were found to be very close while the latter technique took a fraction of time required by the global approach.

REFERENCES

1. Shao, Shaowen; Murotsu, Yoshisada; Structural Reliability analysis using a neural network, Nippon Kikai Gakkai Ronbunshu, A Hen/Transactions of the Japan Society of Mechanical Engineers, Part A , v 62, n 603, Nov, 1996, JSME, Tokyo, Japan, p 2628-2634

2. Bucher, C.G.; Bourgund, U.; A Fast and efficient response surface approach for structural reliability problems, Structural Safety , v 7, n 1, Jan, 1990, p 57-66

3. Liu, Ying Wei; Moses, Fred; A Sequential response surface method and its application in the reliability analysis of aircraft structural, Structural Safety , v16, n1-2, Oct, 1994, Elsevier Science Publishers B.V., Amsterdam, Neth, p 39-46

4. Millwater, H.R.; Wu, Y.-T.; Global/local methods for probabilistic structural analysis, Collection of Technical Papers - AIAA/ASME Structures, Structural Dynamics and Materials Conference, 34th AIAA/ASME/ASCE/AHS/ASC Structures, Structural Dynamics and Materials Conference, Apr 19-22 1993, 1993, La Jolla, CA, USA, Publ by AIAA, Washington, USA, p 701-706

5. Wu, Y.-T.; Computational methods for efficient structural reliability and reliability sensitivity analysis, AIAA Journal , v 32, n 8, Aug, 1994, AIAA, Washington, DC, USA, p 1717-1723

6. Torng, T.Y.; Lin, H.-Z.; Khalessi, M.R.; Reliability calculation based on a robust importance sampling method, Collection of Technical Papers - AIAA/ASME/ASCE/AHS Structures, Structural Dynamics & Materials Conference, Proceedings of the 1996 37th AIAA/ASME/ASCE/AHS/ASC Structures, Structural Dynamics, and Materials Conference. Part 3 (of 4), Apr 15-17 1996, 1996, Salt Lake City, UT, USA, p 1316-1325

7. Bucher, Christian G.; Adaptive sampling an interative fast Monte Carlo procedure, Structural Safety , v 5, n 2, Jun, 1988, p 119-126

8. Southwest Research Institute, NESSUS, San Antonio, Texas, 1991

9. Veritas Sesam Systerms, PROBAN, Hoston, Texas, 1991

10. Liu, P.-L.; A. Der Kiureghian; Optimization algorithms for structural reliability analysis, Report UCB/SESM-86/09, Berkeley, California, 1986

11. Khalessi, M.R.; Lin, H.-Z.; Trent, D.J.; Development of the FEBRELTM finite element-based reliability computer program, Collection of Technical Papers - AIAA/ASME Structures, Structural Dynamics and Materials Conference, 34th AIAA/ASME/ASCE/AHS/ASC Structures, Structural Dynamics and Materials Conference, Apr 19-22 1993, 1993, La Jolla, CA, p 753-761

12. Estes, Allen C.; Frangopol, Dan M.; RELSYS: A computer program for structural system reliability, Structural Engineering and Mechanics , v 6, n 8, Dec, 1998, Techno- Press, Taejon, South Korea, p 901-919

13. Nikolaidis, Efstratios; Burdisso, Ricardo; Reliability based optimization: a safety index approach, Computers and Structures , v 28, n 6, 1988, p 781-788

14. Torng, T.Y.; Yang, R.J.; An Advanced reliability based optimization method for robust structural system design, Collection of Technical Papers - AIAA/ASME Structures, Structural Dynamics and Materials Conference, 34th AIAA/ASME/ASCE/AHS/ASC Structures, Structural Dynamics and Materials Conference, Apr 19-22 1993, 1993, La Jolla, CA, p 1198-1206

15. Wang, Liping; Grandhi, Ramana V.; Hopkins, Dale A.; Structural reliability optimization using an efficient safety index calculation procedure, International Journal for Numerical Methods in Engineering , v38, n10, May 30, 1995, John Wiley & Sons Ltd, Chichester, Engl, p 1721-1738

16. Chandu, Swamy V.L.; Grandhi, Ramana V.; General purpose procedure for reliability based structural optimization under parametric uncertainties, Advances in Engineering Software , v23, n1, 1995, Elsevier Science Ltd, Oxford, Engl, p 7-14

17. Hendawi, Samer; Frangopol, Dan M.; Design of composite hybrid plate girder bridges based on reliability and optimization, Structural Safety , v 15, n 1-2, Aug, 1994, Elsevier Science Publishers B.V., Amsterdam, Neth, p 149-165

18. Tu, J.; Choi, K.K.; Park, Y.H.; A New study on reliability-based design optimization, Journal of Mechanical Design, Transactions of the ASME , v121, n4, Dec, 1999, ASME, Fairfield, NJ, USA, p 557-564

19. Yang, L.; Ma, Z.K.; Optimum design based on reliability for a composite structural system, Computers and Structures , v 36, n 5, 1990, p 785-790

20. Ragon, S.A.; Gurdal, Z.; Haftka, R.T.; Tzong, T.J.; Global/local structural wing design using response surface techniques, Collection of Technical Papers - AIAA/ASME/ASCE/AHS/ASC Structures, Structural Dynamics & Materials Conference, Proceedings of the 1997 38th AIAA/ASME/ASCE/AHS/ASC Structures, Structural Dynamics, and Materials Conference. Part 2 (of 4), Apr 7-10 1997, 1997, Kissimmee, FL, USA, p 1204-1214

21. Liaw, Leslie D.; DeVries, Richard I.; Reliability-based optimization for robust design, International Journal of Vehicle Design , v25, n1-2, 2001, Inderscience Enterprises Ltd, Geneve-15, Switzerland, p 64-77

22. Sevant, Natasha E.; Bloor, Malcolm I.G.; Aerodynamic design of a flying wing using response surface methodology, Journal of Aircraft , v37, n4, Jul, 2000, AIAA, Reston, VA, USA, p 562-569

23. SAS Institute Inc., SAS Version 8.0, 2000

24. Zhou, J.H.; Nowak, A.S.; Integration formulas to evaluate functions of random variables, Structural Safety, v5, n4, Dec, 1988, p 267-284

25. Jaunky, N.; Knight, N.; An assessment of shell theories for buckling of cylindrical panels, International Journal of Solid Structures, Vol. 36, 1999, p 3799-3820

26. Lockheed Martin Missiles and Space Co., Inc., STAGS, 1994.

27. Materials Sciences Corporation, University of Delaware, Army Research Laboratory; The Composite Materials Handbook MIL-17, http://www.mil17.org/

28. Ayyub, B.M.; McCuen, R. H., Probability, statistics, and reliability for engineers, CRC press, 1997

29. Nowak, A. S.; Collins, K. R.; Reliability of structures, McGraw-Hill, 2000.

30. Vanderplaats Research and Development, Inc., DOT- Design Optimization Tools, 1999

31. Bryan Dodson, B.; Nolan, D.; Reliability engineering handbook, Quality Publishing, 1999

APPENDIX A

MONTE CARLO SIMULATION

Monte Carlo (MC) methods are stochastic techniques--meaning they are based on the use of random numbers and probability statistics to investigate problems. MC methods have been used widely from economics to nuclear physics to regulating the flow of traffic. Generally speaking, to call something a "Monte Carlo" experiment, all you need to do is use random numbers to examine some problem.

The procedure for finding the random values for each experiment is described as follows.

An equation to generate random numbers with a normal distribution can be found in the "Reliability Engineering Handbook[31]"

$$x_1 = [\sqrt{-2\ln r_1}\cos(2\pi r_2)]\sigma + \mu$$
$$x_2 = [\sqrt{-2\ln r_1}\sin(2\pi r_2)]\sigma + \mu \qquad \text{(A.1)}$$

Given two uniform random numbers $r_1, r_2 (0 \le r_1, r_2 < 1)$, two normally distributed random numbers with a mean μ and a standard deviation σ will be generated using the above equation. The uniform random numbers r_1 and r_2 could be achieved from a Fortran library routine "r = RAN(I)", where I is an integer as an input and r is a real number as the output.

For example, to get a series of random ply angles with mean μ and standard deviation σ, we choose a pair of uniform random numbers, by applying the above equation we get two ply angles which can be used for two simulations. Then we choose another pair of r_1 and r_2, calculate two ply angles and use them for another two simulations. Use the same method to generate the other ply angles, ply thickness, geometry parameters and material properties.

APPENDIX B

CALCULATION OF HASOFER-LIND RELIABILITY INDEX

The procedure for calculation of reliability index β is described below.

1. Assume an initial value for the design point. It is common to start with the mean values of the basic random variables. The design point in the reduced coordinates should then be computed using

$$X_i'^{*} = \frac{X_i - \mu_{X_i}}{\sigma_{X_i}} \quad \text{for } i = 1,2, \ldots, n \tag{B.1}$$

2. Evaluate the directional cosines at the failure point. The partial derivatives that are needed for computing the directional cosines can be obtained as

$$\left(\frac{\partial g}{\partial X_i'}\right)_* = \left(\frac{\partial g}{\partial X_i}\frac{\partial X_i}{\partial X_i'}\right)_* = \left(\frac{\partial g}{\partial X_i}\right)_* \sigma_{X_i} \quad \text{for i=1,2, …, n} \tag{B.2}$$

3. Solve the following equation for the root β:

$$g\left[\left(\mu_{X_1} - \alpha_1^* \sigma_{X_1}\beta\right), \left(\mu_{X_2} - \alpha_2^* \sigma_{X_2}\beta\right), \cdots, \left(\mu_{X_n} - \alpha_n^* \sigma_{X_n}\beta\right)\right] = 0 \tag{B.3}$$

4. Using the β obtained from step 3, evaluate a new design point using the following equation:

$$X_i^* = \mu_{X_i} - \alpha_i^* \sigma_{X_i}\beta \tag{B.4}$$

5. Repeat steps 1 to 4 until convergence of β is obtained.

The flowchart of this procedure is shown in Fig. B.1.

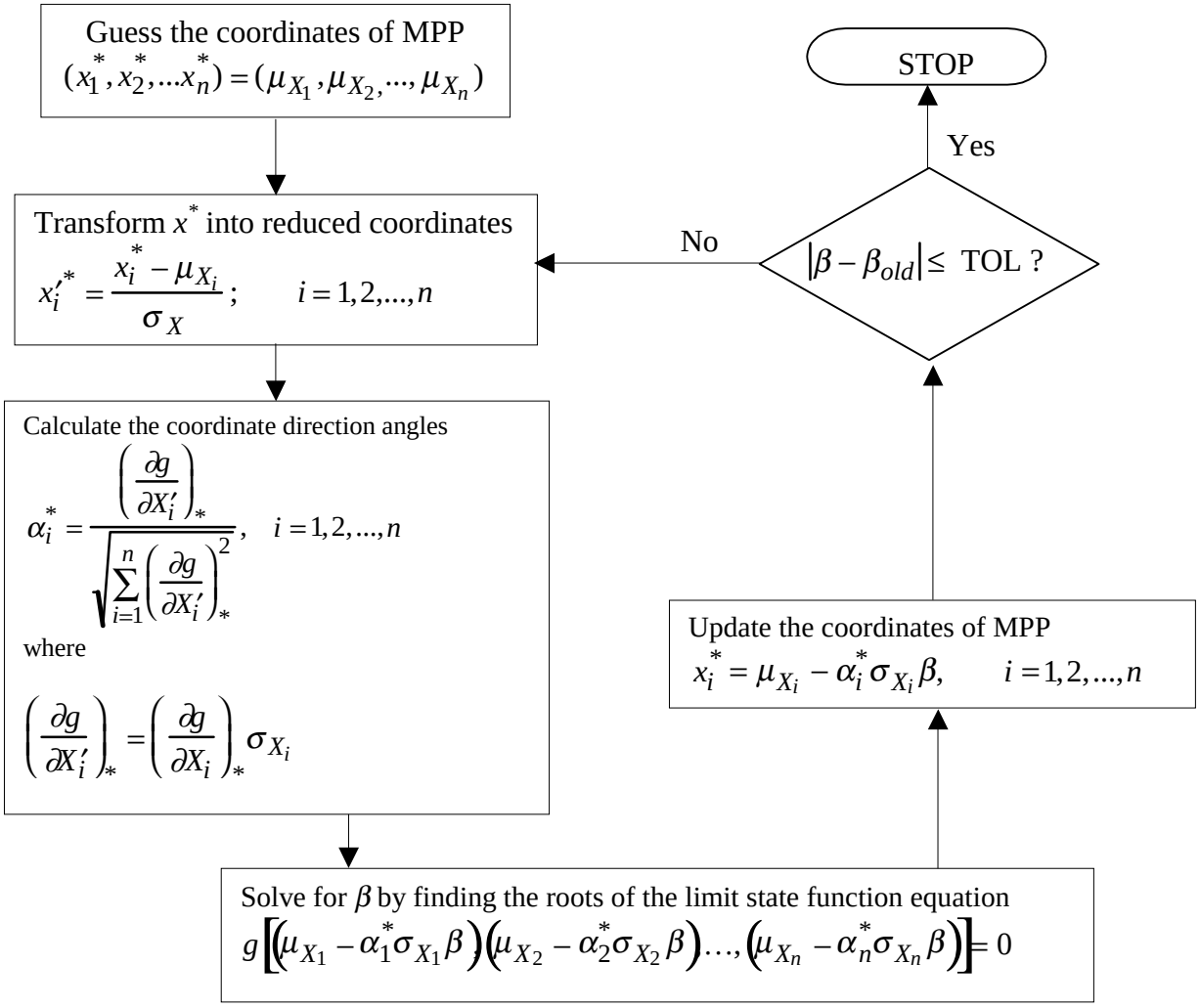

Figure B.1 Flowchart of calculation of safety index β

APPENDIX C

N+1 POINT INTEGRATION SIMULATION

The $n+1$ point integration method is described as follows. All normal random variables are transformed from the standard normal space to general variable space. For each simulation, the *n* general random variables are defined according to the equation

$$x_i = \mu_{X_i} + Z_{i,j}\sigma_{X_i} \quad i,j = 1, 2, \ldots, n \tag{C.1}$$

where the point values to be used for random variables in the first simulation are

$$Z_{1,j} = (z_{1,1}, z_{1,2}, \cdots, z_{1,n}) = (\sqrt{n}, 0, 0, \cdots, 0) \tag{C.2}$$

which means that in the first simulation all random variables are at their mean values except the first random variable which is set to

$$x_1 = \mu_{X_1} + \sqrt{n}\sigma_{X_1} \tag{C.3}$$

In subsequent simulations, the point values are determined as follows

$$Z_{2,j} = \left(-\sqrt{\frac{1}{n}}, \sqrt{\frac{(n+1)(n-1)}{n}}, 0, 0, \cdots, 0 \right) \tag{C.4}$$

$$Z_{3,j} = \left(-\sqrt{\frac{1}{n}}, -\sqrt{\frac{(n+1)}{n(n-1)}}, \sqrt{\frac{(n+1)(n-2)}{(n-1)}}, 0, 0, \cdots, 0 \right) \tag{C.5}$$

$$Z_{4,j} = \left(-\sqrt{\frac{1}{n}}, -\sqrt{\frac{(n+1)}{n(n-1)}}, -\sqrt{\frac{(n+1)}{(n-1)(n-2)}}, \sqrt{\frac{(n+1)(n-3)}{(n-2)}} 0, 0, \cdots, 0 \right) \tag{C.6}$$

$$Z_{n,j} = \left(-\sqrt{\frac{1}{n}}, -\sqrt{\frac{(n+1)}{n(n-1)}}, -\sqrt{\frac{(n+1)}{(n-1)(n-2)}}, \sqrt{\frac{(n+1)}{(n-2)(n-3)}}, \cdots, 0, 0, \cdots, \sqrt{\frac{(n+1)}{2}} \right) \tag{C.7}$$

$$Z_{n+1,j} = \left(-\sqrt{\frac{1}{n}}, -\sqrt{\frac{(n+1)}{n(n-1)}}, -\sqrt{\frac{(n+1)}{(n-1)(n-2)}}, \sqrt{\frac{(n+1)}{(n-2)(n-3)}}, \cdots, 0, 0, \cdots, -\sqrt{\frac{(n+1)}{2}} \right) \tag{C.8}$$